Nuclear Science and Engineering

ISSN: (Print) (Online) Journal homepage: https://www.tandfonline.com/loi/unse20

Multidual Sensitivity Method in Ray-Tracing Transport Simulations

Matthew R. Balcer, Harry Millwater & Jeffrey A. Favorite

To cite this article: Matthew R. Balcer, Harry Millwater & Jeffrey A. Favorite (2021) Multidual Sensitivity Method in Ray-Tracing Transport Simulations, Nuclear Science and Engineering, 195:9, 907-936, DOI: 10.1080/00295639.2021.1883949

To link to this article: https://doi.org/10.1080/00295639.2021.1883949

Published online: 01 Jul 2021.

NUCLEAR SCIENCE AND ENGINEERING · VOLUME 195 · 907–936 · SEPTEMBER 2021
DOI: https://doi.org/10.1080/00295639.2021.1883949

Multidual Sensitivity Method in Ray-Tracing Transport Simulations

Matthew R. Balcer,[a] Harry Millwater,[a] and Jeffrey A. Favorite[b]*

[a]*The University of Texas at San Antonio, Department of Mechanical Engineering, San Antonio, Texas 78249*
[b]*Los Alamos National Laboratory, XCP-7, MS F663, Los Alamos, New Mexico 87545*

Received September 22, 2020
Accepted for Publication January 27, 2021

Abstract — *The multidual differentiation method has been implemented in a ray-tracing transport simulation for the purpose of calculating arbitrary-order sensitivities of the uncollided particle leakage. This method extends dual number differentiation by perturbing variables along multiple nonreal axes to calculate arbitrary-order derivatives. Numerical results of first-through third-order multidual sensitivities of the uncollided particle leakage with respect to isotope densities, microscopic cross sections, source emission rates, and material interface locations (including the outer boundary) are shown for a two-region sphere. The relative error of first and second partial derivatives with respect to isotopic parameters and first partial derivatives of the leakage with respect to interface locations are within 9.8E−10% of existing adjoint-based sensitivities. Higher-order multidual-based derivatives that are not available with the adjoint method are in excellent agreement with central difference approximations.*

Keywords — *Multidual sensitivity, high-order derivatives, ray-tracing transport simulation.*

Note — *Some figures may be in color only in the electronic version.*

I. INTRODUCTION

Incorporating hypercomplex variables and algebra into existing software and numerical algorithms provides a convenient method to compute accurate numerical derivatives. The advantage of this approach is that the real-variable algorithms and software require minimal alterations, that is, no new formulations must be developed and programmed. In general, the existing real variables of interest are "uplifted" to hypercomplex, then perturbed along nonreal axes. Computation of the existing, but now hypercomplex, numerical algorithms yields the traditional results in the real part of the output and derivatives in the nonreal parts.

Hypercomplex numbers contain a single real part and multiple nonreal parts. Two types of hypercomplex numbers are multicomplex and multidual numbers. The nonreal parts of a multicomplex number are represented by an imaginary number, $i^2 = -1$ (Ref. 1). The nonreal parts of a multidual number are represented by the nonreal component of dual number, $\epsilon^2 = 0$ where $\epsilon \neq 0$ (Ref. 2). Hypercomplex differentiation is an extension of the first-order derivative derived from the complex Taylor series, known as the complex-step method.[3] Higher-order derivatives are derived with hypercomplex algebra as outlined in Ref. 1 using multicomplex variables and in Ref. 2 using multidual variables.

Hypercomplex differentiation has been applied to many fields in engineering. For example, hypercomplex

*E-mail: fave@lanl.gov
This material is published by permission of the CONsortium on Nuclear sECurity Technologies (CONNECT), for the U.S. Department of Energy National Nuclear Security Administration under Contract No. DE-NA0003948.

algebra has been implemented in finite element analysis (FEA) to calculate second-order derivatives of the stiffness matrix for energy release rate sensitivities.[4] A second-order Kalman filter using multicomplex numbers was developed in Ref. 5. Multidual numbers were implemented in a computational fluid dynamics simulation for second-order derivatives of the lift coefficient of an airfoil with respect to angle of attack and Mach number.[2]

In the nuclear engineering field, the complex-step method was applied to verify first derivatives computed with other methods in MATWS, a code that "combines the point-kinetics module from the SAS4A/SASSYS computer code with a simplified representation of a reactor heat-removal system."[6] More recently, Ref. 7 implemented the complex-step method in the neutron transport equation to obtain first-order derivatives of the k-eigenvalue with respect to nuclear cross sections. Also, the dual number differentiation method was used in Ref. 8 to calculate first-order partial derivatives for a sensitivity and uncertainty analysis for a diffusion problem, again for the k-eigenvalue.

While complex and dual variables have been used to compute first-order derivatives,[7,8] this paper computes higher-order derivatives using multidual numbers. This extension is significant. Complex and dual variables involve a single imaginary axis, a concept familiar to engineers and scientists. However, hypercomplex (including multidual) numbers involve multiple imaginary axes defined in a specific manner with formal algebraic rules. Hence, the development of a numerical library to carry out the mathematical operations for hypercomplex numbers requires a significantly greater effort than complex or dual. This paper is the first application of hypercomplex algebra to compute higher-order derivatives within nuclear engineering.

Extremely efficient adjoint-based first derivatives of many responses in transport theory have been available for decades. Adjoint-based second derivatives have recently been derived and implemented[9–11] and even adjoint-based third derivatives are now within reach.[12] The multicomplex or multidual approach will not benefit transport theory unless it can provide something new. Currently, only first and second derivatives for isotopic parameters (which include microscopic cross section, source emission rate, and density) and first derivatives for material interface locations have been numerically calculated with the adjoint method (in this paper, the phrase "interface locations" includes the outer boundary).[11] This paper shows how arbitrary-order partial derivatives are obtained using multidual algebra and describes how this method can be implemented in a transport code.

Methods using higher-order derivatives have been developed in optimization, uncertainty quantification, and surrogate modeling but are often not employed due to the high computational expense of calculating these derivatives. The efficient calculation of higher-order derivatives will allow broader use of second-order optimization methods including Newton, conjugate gradient, quasi-Newton, Gauss-Newton, and approximate greatest descent and third-order optimization techniques, such as the Halley method.[13,14] Taylor series approximations of probabilistic moments using arbitrary-order derivatives have been available for many years,[15] and applications of these equations are increasingly being explored since high-order derivatives are becoming more available. For example, a second-order sensitivity study of the uncollided leakage found that the second-order derivative term was the only contributing term for skewness.[9] High-order Taylor series surrogate models are also being used in engineering. Reference 16 showed that a probability density function produced from the sampling of a fourth-order Taylor series surrogate model agreed well with sampling from an FEA model for a ten-bar truss system.

The multidual differentiation method is presented in Sec. II. An overview of the ray-tracing transport method is presented in Sec. III. The multidual differentiation method is applied to a two-region sphere in Sec. IV. A summary of this work as well as a discussion of the capabilities and limitations of the multidual sensitivity method is given in Sec. V.

II. MULTIDUAL ALGEBRA TO COMPUTE AN ARBITRARY-ORDER PARTIAL DERIVATIVE

The second-order partial derivative using multidual numbers derived in Ref. 2 (the term "hyper-dual" numbers in Ref. 2 is the same as multidual numbers in this paper) is summarized here and then extended to arbitrary-order partial derivatives. Section II.A describes how first derivative expressions are derived from a real, imaginary, or dual step in the Taylor series expansion (TSE). The method is then extended to multidual number steps for second- and higher-order derivative expressions in Sec. II.B. The implementation of the multidual sensitivity method in code is discussed in Sec. II.C.

II.A. First-Order Partial Derivative Expressions

Expressions for partial derivatives can be derived through the TSE of an analytic function f that depends on a real variable x with a step or perturbation of size h applied to x. This TSE is expressed as

$$f(x+h) = f(x) + hf'(x) + \frac{1}{2!}h^2 f''(x) + \frac{1}{3!}h^3 f'''(x) + \ldots . \quad (1)$$

The choice of h in Eq. (1) can lead to different derivative expressions. Finite difference approximations can be derived when h is a real number. For example, the forward difference approximation of the first derivative is derived from Eq. (1) by solving for $f'(x)$, which gives

$$f'(x) = \frac{f(x+h) - f(x)}{h} + O(h) \ . \tag{2}$$

Finite difference approximations require multiple function evaluations and contain subtractive cancellation error and truncation error.[17] A convergence study is traditionally needed to find the "optimal" step size h, although methods for obtaining "near optimum" step sizes exist.[18] However, this method requires knowledge of the second derivative. Applying the step in a nonreal direction alleviates these limitations.

An imaginary step ih in Eq. (1) leads to an approximation of the first derivative, known as the complex-step derivative approximation.[3,19] This TSE becomes

$$f(x+ih) = f(x) + ihf'(x) - \frac{1}{2!}h^2 f''(x) - i\frac{1}{3!}h^3 f'''(x) + \ldots \ , \tag{3}$$

where the imaginary number i is defined as $i^2 = -1$. Taking the imaginary part, denoted by $Im[\cdot]$, of Eq. (3) and dividing both sides by h gives an approximation to the first partial derivative:

$$f'(x) = \frac{Im[f(x+ih)]}{h} + O(h^2) \ . \tag{4}$$

When h is sufficiently small, usually on the order of 10^{-10} times the variable of interest, the complex-step derivative approximation gives results with machine accuracy.[3,19]

Alternatively, a dual number can be used for the nonreal step. Dual numbers are a subset of generalized complex numbers.[20,21] A dual number has the form $a + \epsilon b$, where a and b are real numbers and ϵ represents the nonreal component. The nonreal component of a dual number is defined under the constraint that $\epsilon^2 = 0$, which implies $\epsilon^p = 0$ for $p \geq 2$, and $\epsilon \neq 0$. Extraction of the nonreal part of a dual number is denoted by ϵ part $[a + \epsilon b] = b$. A dual step, ϵh, in Eq. (1) gives

$$f(x + \epsilon h) = f(x) + \epsilon h f'(x) + \cancelto{0}{\epsilon^2}\frac{1}{2!}h^2 f''(x) + \cancelto{0}{\epsilon^3}\frac{1}{3!}h^3 f'''(x) + \cdots \ , \tag{5}$$

which truncates exactly at the first derivative. The first derivative $f'(x)$ is found by taking the nonreal part of both sides of Eq. (5) and dividing by step size h, which gives

$$f'(x) = \frac{\epsilon \text{ part } [f(x+\epsilon h)]}{h} \ . \tag{6}$$

The dual step derivative in Eq. (6) has no subtraction cancellation error, similar to the complex-step derivative approximation in Eq. (4). It also has no truncation error and therefore has no dependence on the step size h. In practice, a step size of $h = 1$ is chosen so that h can be omitted from Eq. (6).

II.B. Second- and Higher-Order Partial Derivative Expressions Using Multidual Numbers

The derivation of second-order partial derivatives using multidual algebra in Ref. 2 is summarized here and then generalized to arbitrary-order partial derivatives of functions with multiple variables. Consider a multidual number with three nonreal parts where ϵ_1, ϵ_2, and $\epsilon_1\epsilon_2$, are the first, second, and third nonreal parts, respectively, and $\epsilon_1\epsilon_2 = \epsilon_2\epsilon_1$. These nonreal components are defined under the constraints $\epsilon_1^2 = \epsilon_2^2 = (\epsilon_1\epsilon_2)^2 = 0$, $\epsilon_1 \neq 0$, $\epsilon_2 \neq 0$, and $\epsilon_1\epsilon_2 \neq 0$.

A multidual step with a perturbation in the ϵ_1 and ϵ_2 nonreal directions of sizes h_1 and h_2, respectively, and zero perturbation in the $\epsilon_1\epsilon_2$ direction in Eq. (1) reduces to

$$\begin{aligned} f(x + \epsilon_1 h_1 + \epsilon_2 h_2 + 0\epsilon_1\epsilon_2) &= f(x) + \epsilon_1 h_1 f'(x) + \epsilon_2 h_2 f'(x) \\ &\quad + \epsilon_1\epsilon_2 h_1 h_2 f''(x) \, , \end{aligned} \tag{7}$$

which truncates exactly at the second derivative. An expression for the second derivative is derived from Eq. (7) by taking the $\epsilon_1\epsilon_2$ part and dividing by h_1h_2, which gives

$$f''(x) = \frac{d^2 f(x)}{dx^2} = \frac{\epsilon_1\epsilon_2 \text{ part}[f(x + \epsilon_1 h_1 + \epsilon_2 h_2 + 0\epsilon_1\epsilon_2)]}{h_1 h_2} \ . \tag{8}$$

The second derivative using a multidual step in Eq. (8) contains no truncation error and therefore does not depend on step sizes h_1 or h_2. The step sizes can be omitted from Eq. (8) when $h_1 = 1$ and $h_2 = 1$.

Partial derivatives of a function of m variables $f(\boldsymbol{x})$, where $\boldsymbol{x} = [x_1, \ldots, x_i, \ldots, x_j, \ldots, x_m]$, can be calculated by applying a nonreal step to each variable of interest. For example, a second partial derivative of $f(\boldsymbol{x})$ with Respect to the variables x_i and x_j, $\partial^2 f(\boldsymbol{x})/\partial x_i \partial x_j$, can be found by applying a step to each variable in different nonreal directions. A TSE of $f(\boldsymbol{x})$ with the step $\epsilon_1 h_1 \boldsymbol{e}_i + \epsilon_2 h_2 \boldsymbol{e}_j + 0\epsilon_1\epsilon_2$ reduces to

$$\begin{aligned} f\left(\boldsymbol{x} + \epsilon_1 h_1 \boldsymbol{e}_i + \epsilon_2 h_2 \boldsymbol{e}_j + 0\epsilon_1\epsilon_2\right) &= f\left(x_1, \ldots, x_i + \epsilon_1 h_1, \ldots, x_j + \epsilon_2 h_2, \ldots, x_m\right) \\ &= f(\boldsymbol{x}) + \epsilon_1 h_1 \frac{\partial f(\boldsymbol{x})}{\partial x_i} + \epsilon_2 h_2 \frac{\partial f(\boldsymbol{x})}{\partial x_j} \\ &\quad + \epsilon_1\epsilon_2 h_1 h_2 \frac{\partial^2 f(\boldsymbol{x})}{\partial x_i \partial x_j} \ , \end{aligned} \tag{9}$$

where $\boldsymbol{e}_i$ and $\boldsymbol{e}_j$ are unit vectors with a value of one in the i'th and j'th positions, respectively, and zeros elsewhere. These unit vectors indicate the variables in $\boldsymbol{x}$ that the steps are applied to. The first derivatives $\partial f(\boldsymbol{x})/\partial x_i$ and $\partial f(\boldsymbol{x})/\partial x_j$ are found by taking the ϵ_1 part and the ϵ_2 part of Eq. (9), respectively, and dividing by the appropriate step size, h_1 or h_2. The second derivative $\partial^2 f(\boldsymbol{x})/\partial x_i \partial x_j$ is found by taking the $\epsilon_1\epsilon_2$ part of Eq. (9) and dividing by $h_1 h_2$. This gives

$$\frac{\partial f(\boldsymbol{x})}{\partial x_i} = \frac{\epsilon_1 \operatorname{part}\left[f\left(\boldsymbol{x} + \epsilon_1 h_1 \boldsymbol{e}_i + \epsilon_2 h_2 \boldsymbol{e}_j + 0\epsilon_1\epsilon_2\right)\right]}{h_1} \ , \tag{10}$$

$$\frac{\partial f(\boldsymbol{x})}{\partial x_j} = \frac{\epsilon_2 \operatorname{part}\left[f\left(\boldsymbol{x} + \epsilon_1 h_1 \boldsymbol{e}_i + \epsilon_2 h_2 \boldsymbol{e}_j + 0\epsilon_1\epsilon_2\right)\right]}{h_2} \ , \tag{11}$$

and

$$\frac{\partial^2 f(\boldsymbol{x})}{\partial x_i \partial x_j} = \frac{\epsilon_1\epsilon_2 \operatorname{part}\left[f\left(\boldsymbol{x} + \epsilon_1 h_1 \boldsymbol{e}_i + \epsilon_2 h_2 \boldsymbol{e}_j + 0\epsilon_1\epsilon_2\right)\right]}{h_1 h_2} \ , \tag{12}$$

which are equivalent to the expressions presented in Ref. 2.

Furthermore, an expression for an n'th-order partial derivative of $f(\boldsymbol{x})$ can be derived using a multidual number with $2^n - 1$ nonreal parts. A step in different nonreal directions is applied to each variable of interest. The resulting n'th-order partial derivative of $f(\boldsymbol{x})$ is

$$\frac{\partial^n f(\boldsymbol{x})}{\partial x_i \cdots \partial x_k} = \frac{\epsilon_1 \cdots \epsilon_n \operatorname{part}[f(\boldsymbol{x} + \epsilon_1 h_1 \boldsymbol{e}_i + \cdots + \epsilon_n h_n \boldsymbol{e}_k + \cdots + 0\epsilon_1 \cdots \epsilon_n]}{h_1 \cdots h_n} \ , \tag{13}$$

where $\boldsymbol{e}_i$ through $\boldsymbol{e}_k$ are unit vectors that indicate the variables in $\boldsymbol{x}$ that the step is applied to. The n'th-order partial derivative expression in Eq. (13) has no truncation error and is therefore independent of step sizes h_i. It is convenient to choose all step sizes equal to one so they can be omitted from Eq. (13):

$$\frac{\partial^n f(\boldsymbol{x})}{\partial x_i \cdots \partial x_k} = \epsilon_1 \cdots \epsilon_n \operatorname{part}\left[f(\boldsymbol{x} + \epsilon_1 \boldsymbol{e}_i + \cdots + \epsilon_n \boldsymbol{e}_k + \cdots + 0\epsilon_1 \cdots \epsilon_n)\right] \ . \tag{14}$$

Lower-order partial derivatives can be obtained from the same function evaluation in Eq. (14) by taking different nonreal parts. For example, the third-order partial derivative, $\partial^3 f(\boldsymbol{x})/\partial x_i \partial x_j \partial x_k$, can be obtained from Eq. (14) using $n = 3$ which gives

$$\frac{\partial^3 f(\boldsymbol{x})}{\partial x_i \partial x_j \partial x_k} = \epsilon_1\epsilon_2\epsilon_3 \operatorname{part}\left[f\left(\boldsymbol{x} + \epsilon_1 h_1 \boldsymbol{e}_i + \epsilon_2 h_2 \boldsymbol{e}_j + \epsilon_3 h_3 \boldsymbol{e}_k + 0\epsilon_1\epsilon_2 + 0\epsilon_1\epsilon_3 + 0\epsilon_2\epsilon_3 + 0\epsilon_1\epsilon_2\epsilon_3\right)\right] \ . \tag{15}$$

Subsequently, first- and second-order partial derivatives can be found from the same function evaluation in Eq. (15) as

$$\frac{\partial^2 f(\boldsymbol{x})}{\partial x_i \partial x_j} = \epsilon_1\epsilon_2 \,\mathrm{part}\left[f\left(\boldsymbol{x} + \epsilon_1\boldsymbol{e}_i + \epsilon_2\boldsymbol{e}_j + \epsilon_3\boldsymbol{e}_k + 0\epsilon_1\epsilon_2 + 0\epsilon_1\epsilon_3 + 0\epsilon_2\epsilon_3 + 0\epsilon_1\epsilon_2\epsilon_3\right)\right] \quad , \tag{16}$$

$$\frac{\partial^2 f(\boldsymbol{x})}{\partial x_i \partial x_k} = \epsilon_1\epsilon_3 \,\mathrm{part}\left[f\left(\boldsymbol{x} + \epsilon_1\boldsymbol{e}_i + \epsilon_2\boldsymbol{e}_j + \epsilon_3\boldsymbol{e}_k + 0\epsilon_1\epsilon_2 + 0\epsilon_1\epsilon_3 + 0\epsilon_2\epsilon_3 + 0\epsilon_1\epsilon_2\epsilon_3\right)\right] \quad , \tag{17}$$

$$\frac{\partial^2 f(\boldsymbol{x})}{\partial x_j \partial x_k} = \epsilon_2\epsilon_3 \,\mathrm{part}\left[f\left(\boldsymbol{x} + \epsilon_1\boldsymbol{e}_i + \epsilon_2\boldsymbol{e}_j + \epsilon_3\boldsymbol{e}_k + 0\epsilon_1\epsilon_2 + 0\epsilon_1\epsilon_3 + 0\epsilon_2\epsilon_3 + 0\epsilon_1\epsilon_2\epsilon_3\right)\right] \quad , \tag{18}$$

$$\frac{\partial f(\boldsymbol{x})}{\partial x_i} = \epsilon_1 \,\mathrm{part}\left[f\left(\boldsymbol{x} + \epsilon_1\boldsymbol{e}_i + \epsilon_2\boldsymbol{e}_j + \epsilon_3\boldsymbol{e}_k + 0\epsilon_1\epsilon_2 + 0\epsilon_1\epsilon_3 + 0\epsilon_2\epsilon_3 + 0\epsilon_1\epsilon_2\epsilon_3\right)\right] \quad , \tag{19}$$

$$\frac{\partial f(\boldsymbol{x})}{\partial x_j} = \epsilon_2 \mathrm{part}\left[f\left(\boldsymbol{x} + \epsilon_1\boldsymbol{e}_i + \epsilon_2\boldsymbol{e}_j + \epsilon_3\boldsymbol{e}_k + 0\epsilon_1\epsilon_2 + 0\epsilon_1\epsilon_3 + 0\epsilon_2\epsilon_3 + 0\epsilon_1\epsilon_2\epsilon_3\right)\right] , \tag{20}$$

and

$$\frac{\partial f(\boldsymbol{x})}{\partial x_k} = \epsilon_3 \mathrm{part}[f(\boldsymbol{x} + \epsilon_1\boldsymbol{e}_i + \epsilon_2\boldsymbol{e}_j + \epsilon_3\boldsymbol{e}_k + 0\epsilon_1\epsilon_2 + 0\epsilon_1\epsilon_3 + 0\epsilon_2\epsilon_3 + 0\epsilon_1\epsilon_2\epsilon_3)] \ . \tag{21}$$

A numerical example of calculating derivatives from a multidual step is shown in Appendix A.

II.C. Code Implementation of the Multidual Differentiation Method

The only source code modifications needed to implement the multidual differentiation method are syntax changes, based on the multidual algebra library, and inclusion of Eq. (14) to extract sensitivities of the output. In this work, a spherical ray-tracing transport code[11] was modified to calculate multidual-based derivatives, where multidual algebra is handled by the MultiZ library.[22] With this approach, traditional mathematical operations are overloaded by the MultiZ library to use multidual algebra.

The implementation of multidual differentiation in existing code is general. The following description applies to procedural programming languages such as Fortran or C, but can be extended to object-oriented languages like Python or C++. A detailed description of the multidual algebra library used here, MultiZ, is given in Ref. 22. For all variables of interest, real-valued variable types are transformed to multidual types. That is, a real number is declared as a multidual number, a vector is declared as a multidual vector, and a matrix is declared as a multidual matrix. Similarly, any functions that use these variables are also declared as multidual. All remaining variables are left unchanged. Multidual vectors and matrices are then allocated based on the number of nonreal parts of the multidual step. The external library handles array indexing so an interface, defined in the external library, is called when assigning or retrieving positions of arrays. A nonreal step is applied to each variable of interest where they are first calculated, following Eq. (14). Finally, sensitivities are calculated by extracting nonreal parts of the output using Eq. (14). A numerical example of a multidual code conversion is shown in Appendix A.

The minimum number of nonreal parts in a multidual step is $2^n - 1$ for an n'th-order partial derivative calculation. So, a separate function evaluation is needed for each n'th-order partial derivative with a multidual step containing the minimum number of nonreal parts. The function can be placed inside a loop where different steps are applied to the appropriate variables on each run for each n'th-order partial derivative calculation. Algorithms that leverage lower-order derivative calculations from a higher-order multidual step may be developed; see Eqs. (15) through (21). However, the number of multidual algebraic operations grows rapidly with the number of nonreal parts, which will increase computational memory and run time.

III. APPLICATION TO UNCOLLIDED TRANSPORT (RAY TRACING)

Photopeaks in a gamma-ray spectrum may be calculated by assuming that there is no scattering into the peak and that a simple detector efficiency curve converts particles entering the detector to counts in the peak. Under these assumptions, there is no scattering in the transport equation, and the leakage of uncollided particles or the flux of uncollided particles on the boundary becomes the quantity of interest. This simplified transport equation is solved in this work using the deterministic ray-tracing simulation called SENSPG developed by Ref. 23 and described as follows using an example.

Consider the two-region sphere shown in Fig. 1. If only the center region emits gamma rays, the uncollided angular flux $\psi(r_d,\theta)$ at the detector point r_d at angle θ with Respect to the surface normal at r_d is[11,23]

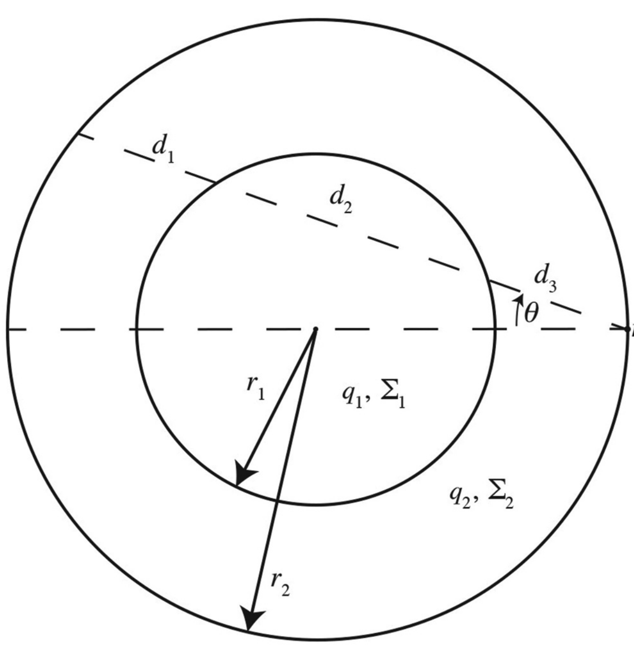

Fig. 1. Ray-tracing in a two-region sphere.

$$\psi(r_d,\theta) = \begin{cases} \frac{q_1}{4\pi\Sigma_1}\left(1-e^{-\Sigma_1 d_2}\right)e^{-\Sigma_2 d_3} & 0 \le \sin(\theta) < \frac{r_1}{r_2} \\ 0 & \frac{r_1}{r_2} < \sin(\theta) \le 1 \end{cases} , \tag{22}$$

where q_k and Σ_k are the source rate density and macroscopic cross section for the material in region k and the other quantities are shown in Fig. 1. These material quantities are computed from isotopic quantities using

$$q_k = \sum_{i=1}^{I} N_i q_{e,i} \tag{23}$$

and

$$\Sigma_k = \sum_{i=1}^{I} N_i \sigma_i \quad , \tag{24}$$

where N_i is the atom density of nuclide i in region k, and $q_{e,i}$ and σ_i are its source emission rate and microscopic cross section. The total uncollided leakage L is $\cos(\theta)\psi(r_d,\theta)$ integrated over θ (in a spherical coordinate system) and over the surface area[23]:

$$\begin{aligned} L &= \int dS \int_0^{2\pi} d\omega \int_0^{\frac{\pi}{2}} d\theta \sin(\theta)\cos(\theta)\psi(r_d,\theta) \\ &= 2\pi r_2^2 \int_0^{\operatorname{asin}\left(\frac{r_1}{r_2}\right)} d\theta \sin(\theta)\cos(\theta)\frac{q_1}{\Sigma_1}\left(1-e^{-\Sigma_1 d_2(\theta)}\right) \\ &\quad \times e^{-\Sigma_2 d_3(\theta)} \quad , \end{aligned} \tag{25}$$

where it is now explicit that the path lengths d through the regions depend on θ.

The integral in Eq. (25) is analytic only in the case of a one-region homogeneous sphere.[11] In the spherical ray-tracing code SENSPG, the integral is evaluated using the QUADPACK adaptive numerical integration library.[24] Equations (22) and (25) are given in the form specific to Fig. 1 only for ease of presentation. The MultiZ library was implemented for the full generality that SENSPG handles, an arbitrary number of regions with any of them radiating.

IV. TWO-REGION SPHERE NUMERICAL EXAMPLE

The two-region sphere shown in Fig. 1 is used as an example to verify the accuracy of multidual sensitivities. This problem is identical to the two-region sphere example in Ref. 11. The material and geometry of the sphere are given in Table I. The quantity of interest was the total uncollided leakage L of the 646-keV gamma-ray line from the decay of ^{239}Pu. The source emission rate, microscopic cross section, and density of the isotopes in each material are given in Table II (note that photon cross sections depend on nuclide proton number, not isotope). Using these parameters in Eq. (25), the leakage is $L = 7.316561897302186 \times 10^4/\mathrm{s}$.

The first derivatives of L with respect to nuclide densities, microscopic total cross sections, source emission rates, and interface locations were computed using the multidual method and compared to the adjoint-based results presented in Ref. 11 (except that 16 digits are used in this paper). All of the first derivatives matched to within 1.959E−10%. The adjoint-based first derivatives for these parameters have been available for decades, so the multidual approach does not provide any benefit here. However, the comparison must be made to verify the multidual differentiation approach.

The second derivatives of L with respect to nuclide densities, microscopic total cross sections, and source emission rates, including mixed partial derivatives, were computed using the multidual method and compared to the adjoint-based results presented in Ref. 11 (except that 16 digits are used in this paper). All of the second derivatives matched to within 9.796E−10%. These second derivatives have only recently become available[9,10] and may not yet be widespread, so there is value in showing that the multidual approach can compute them.

Multidual-based derivatives that are currently not available with adjoint methods are compared to central difference results using lower-order adjoint derivatives. The central difference formulas used in this paper are described as follows. A second derivative of a function $f(\boldsymbol{x})$, where $\boldsymbol{x} = [x_1, \ldots, x_i, \ldots, x_j, \ldots, x_k, \ldots, x_m]$, can be approximated from the central difference of first derivatives as

$$\frac{\partial^2 f(\boldsymbol{x})}{\partial x_i \partial x_j} \approx \frac{\left.\frac{\partial f(\boldsymbol{x})}{\partial x_j}\right|_{x_{i0}+h_i, x_{j0}} - \left.\frac{\partial f(\boldsymbol{x})}{\partial x_j}\right|_{x_{i0}-h_i, x_{j0}}}{2h_i} , \tag{26}$$

where subscript 0 denotes the initial value of the variable and h_i is the step size of variable x_i. Similarly, third derivatives can be approximated by the central difference of second derivatives as

$$\frac{\partial^3 f(\boldsymbol{x})}{\partial x_i \partial x_j \partial x_k} \approx \frac{\left.\frac{\partial^2 f(\boldsymbol{x})}{\partial x_j \partial x_k}\right|_{x_{i0}+h_i, x_{j0}, x_{k0}} - \left.\frac{\partial^2 f(\boldsymbol{x})}{\partial x_j \partial x_k}\right|_{x_{i0}-h_i, x_{j0}, x_{k0}}}{2h_i} . \tag{27}$$

TABLE I

Two-Region Sphere Geometry and Material Composition

Region	Outer Radius r_i (cm)	Mass Density ρ (g/cm^3)	Source Rate Density q (/cm^3/s)	Macroscopic Cross Section Σ (/cm)
1	3.794	19.6	6.21093352×10^3	2.59960753
2	7.604	0.95	0.	0.08442073

TABLE II

Two-Region Sphere Nuclide Parameters

Region	Isotope	Concentration (wt%)	Cross Section σ_i (b)	Source Emission Rate q_i [γ/(10^{24} atoms)/s]	Density N_i (atom/b · cm)
1	^{239}Pu	93.8039	52.726316	1.341×10^5	4.6315686×10^{-2}
	^{240}Pu	5.94113	52.726316	0.	2.9211935×10^{-3}
	^{69}Ga	0.1516	8.1738625	0.	2.5946453×10^{-4}
	^{71}Ga	0.103465	8.1738625	0.	1.7218521×10^{-4}
2	C	85.6299	1.5523511	0.	4.0786121×10^{-2}
	^{1}H	14.3701	0.2587445	0.	8.1572189×10^{-2}

When second derivatives are not available directly, second derivative approximations from Eq. (26) are substituted into Eq. (27) for a third-order derivative estimate.

Second derivatives of L with respect to material interface locations and isotopic parameters were computed using the multidual differentiation method; these are shown in Tables III through VI for all nonzero values. Multidual-based derivatives are compared to central difference approximations using Eq. (26) with first-order adjoint-based derivatives. The indices of the derivatives in Tables III through VI match the indices in Eq. (26). A step size of $h_i = 0.1\% \cdot r_i$ was used for the central difference approximations and all multidual step sizes were one. The second-order multidual sensitivities are in excellent agreement with central difference approximations.

Third- and higher-order derivatives are currently not available with the adjoint method. However, these

TABLE III

Second Derivatives of L with Respect to r_i and r_j

Surface		$\partial^2 L/\partial r_i \partial r_j$ (/s · cm^2)		
i	j	Multidual	Central Difference	Difference (%)
r_1	r_1	1.737270423039880E+04	1.737270771332521E+04	2.005E−05
	r_2	−4.280893845549177E+03	−4.280895807775678E+03	−4.584E−05
r_2	r_2	7.255130923984784E+02	7.255138269711493E+02	1.012E−04

TABLE IV

Second Derivatives of L with Respect to r_i and q_j

Surface	Isotope	$\partial^2 L/\partial r_i \partial q_j$ [(10^{24} atoms)/cm · γ]		
i	j	Multidual	Central Difference	Difference (%)
r_1	^{239}Pu	3.324652940606935E−01	3.324652940605137E−01	5.408E−11
r_2	^{239}Pu	−4.923412538429708E−02	−4.92341253843092E−02	−2.469E−11

TABLE V

Second Derivatives of L with Respect to r_i and N_j

Surface	Isotope	$\partial^2 L/\partial r_i \partial N_j$ (b/s · atom)		
i	j	Multidual	Central Difference	Difference (%)
r_1	^{239}Pu	5.899361595961223E+04	5.899362953484812E+04	2.301E−05
	^{240}Pu	−9.036088974934673E+05	−9.036091041516350E+05	−2.287E−05
	^{69}Ga	−1.400813757862801E+05	−1.400814078233294E+05	−2.287E−05
	^{71}Ga	−1.400813757862801E+05	−1.400814078233294E+05	−2.287E−05
	C	−2.069732005259526E+05	−2.069730445681837E+05	−7.535E−05
	^{1}H	−3.449810693552834E+04	−3.449808094062808E+04	−7.535E−05
r_2	^{239}Pu	−9.950162454585119E+03	−9.950164908246586E+03	−2.466E−05
	^{240}Pu	1.325997327953430E+05	1.325997618014447E+05	2.187E−05
	^{69}Ga	2.055618647668205E+04	2.055619097333254E+04	2.187E−05
	^{71}Ga	2.055618647668205E+04	2.055619097333254E+04	2.187E−05
	C	−7.461936134018205E+04	−7.461940268648959E+04	−5.541E−05
	^{1}H	−1.243748804402165E+04	−1.243749493558709E+04	−5.541E−05

TABLE VI

Second Derivatives of L with Respect to r_i and σ_j

Surface	Isotope	$\partial^2 L/\partial r_i \partial \sigma_j$ (/s · cm · b)		
i	j	Multidual	Central Difference	Difference (%)
r_1	^{239}Pu	−7.937453106117697E+02	−7.937454921437886E+02	−2.287E−05
	^{240}Pu	−5.006260007963084E+01	−5.006261152910263E+01	−2.287E−05
	^{69}Ga	−4.446630713693612E+00	−4.446631730651898E+00	−2.287E−05
	^{71}Ga	−2.950862016653879E+00	−2.950862691525268E+00	−2.287E−05
	C	−5.437966929909634E+03	−5.437962832310413E+03	−7.535E−05
	^{1}H	−1.087592678667889E+04	−1.087591859148628E+04	−7.535E−05
r_2	^{239}Pu	1.164778438842654E+02	1.164778693637194E+02	2.187E−05
	^{240}Pu	7.346416587987573E+00	7.346418195010957E+00	2.187E−05
	^{69}Ga	6.525190777900678E−01	6.525192205281520E−01	2.187E−05
	^{71}Ga	4.330230877646499E−01	4.330231824881509E−01	2.187E−05
	C	−1.960532176473768E+03	−1.960533262797245E+03	−5.541E−05
	^{1}H	−3.921061802891702E+03	−3.921063975537121E+03	−5.541E−05

derivatives can be easily obtained with the multidual sensitivity method using Eq. (14). All nonzero third-order partial derivatives of the leakage for the two-region sphere are compared to central differences using lower-order adjoint derivatives; these are shown in Appendix B. High-order derivatives are difficult to obtain with finite differences. Nevertheless, the agreement is excellent.

V. DISCUSSION AND CONCLUSIONS

Multidual algebra was successfully implemented in a ray-tracing transport code to calculate accurate high-order sensitivities of the uncollided particle leakage which have yet to be obtained numerically by adjoint-based differentiation. New high-order derivatives can lead to better approximations for uncertainty analyses, perturbation methods, optimization, inverse problems, surrogate models, and many other applications. Second- and third-order adjoint-based sensitivity methods are only now being developed for transport theory.[9–12] For the many cases in which adjoint-based derivatives are not available, this paper has shown that the multidual approach can be used.

The complex- and dual-step differentiation methods have been implemented in many areas, including nuclear engineering, for first-order derivative calculations.[7,8] Multidual differentiation is a major extension of complex- and dual-step differentiation because it allows one to compute *arbitrary-order* sensitivities with machine precision. However, this method requires multidual variables with multiple imaginary axes and a requisite numerical library to support multidual algebraic operations.

This work applied the multidual differentiation method to a relatively simple ray-tracing code. However, the methodology is general and should be equally applicable to other nuclear applications. The numerical accuracy along with minimal modifications to existing codes make this method attractive for practical applications. The multidual transformation of many types of code is possible. For example, multidual differentiation was implemented in the QUADPACK adaptive numerical integration library in this work, so that the integrand and limits of integration can accept multidual numbers.

The highest-order multidual-based derivative that can be calculated in a single transport calculation is determined by the number of nonreal steps. Additionally, all combinations of lower-order derivatives are obtained in the same transport calculation. In this work, a third-order derivative was calculated from a single transport simulation by applying steps in three nonreal directions. The simulation was repeated for all combinations of third-order derivatives. Lower-order derivatives were calculated as byproducts. In contrast, all adjoint-based first derivatives are obtained with a total of two transport calculations, and all adjoint-based second derivatives are obtained with an additional number of calculations approximately equal to twice the number of parameters. The details of a particular problem will determine which is more efficient, but efficiency is not the only measure of goodness. There is no adjoint-based second or third derivative with respect to material interface locations, for example.

A multidual implementation in a production deterministic transport code, such as the time-dependent, parallel neutral particle transport code system PARTISN (Ref. 25), is the next natural step. Additional work includes the implementation of the multidual sensitivity method in a Monte Carlo transport code. It took the authors one month to fully implement the multidual differentiation method in the simple ray-tracing transport code SENSPG, so the effort to implement the method in a production-level code may be possible. Also, multidual implementation in a code with high complexity leads to greater computational time due to the additional algebraic operations needed for multidual numbers. Despite these limitations, the multidual sensitivity method can still be beneficial by providing higher-order derivatives with machine accuracy.

APPENDIX A

MULTIDUAL DIFFERENTIATION CODE IMPLEMENTATION EXAMPLE

This appendix shows an example of converting a real-valued code to multidual and calculating multidual-based derivatives, as outlined in Sec. II.C. A simple Fortran 77 program to calculate the function

$$f(\boldsymbol{x}) = e^{x_2}\sin(x_1 x_2) \quad , \tag{A.1}$$

with input values $\boldsymbol{x} = [x_1, x_2] = [2, 3]$ is shown as

```
program main
  implicit none
  ! declare variables
  real*8 x(2) ! input: real vector
  real*8 f    ! output: real number
  ! assign input
  x(1) = 2.0d0
  x(2) = 3.0d0
  ! calculate output
  f = exp(x(2))*sin(x(1)*x(2))
end program
```

The result of the function evaluation from this real-valued code is $f(\boldsymbol{x}) = -5.612210305985402$.

First through third partial derivatives are calculated using Eq. (14) with a multidual step with $2^6 - 1$ nonreal parts as

$$\frac{\partial f(\boldsymbol{x})}{\partial x_1} = \epsilon_1 \mathrm{part}[f(\boldsymbol{x} + (\epsilon_1+\epsilon_2+\epsilon_3)\boldsymbol{e}_1 + (\epsilon_4+\epsilon_5+\epsilon_6)\boldsymbol{e}_2 + \cdots + 0\epsilon_1\epsilon_2\epsilon_3\epsilon_4\epsilon_5\epsilon_6)] \quad , \tag{A.2}$$

$$\frac{\partial f(\boldsymbol{x})}{\partial x_2} = \epsilon_4 \,\mathrm{part}\,[f(\boldsymbol{x} + (\epsilon_1+\epsilon_2+\epsilon_3)\boldsymbol{e}_1 + (\epsilon_4+\epsilon_5+\epsilon_6)\boldsymbol{e}_2 + \cdots + 0\epsilon_1\epsilon_2\epsilon_3\epsilon_4\epsilon_5\epsilon_6)] \quad , \tag{A.3}$$

$$\frac{\partial^2 f(\boldsymbol{x})}{\partial x_1^2} = \epsilon_1\epsilon_2 \,\mathrm{part}\,[f(\boldsymbol{x} + (\epsilon_1+\epsilon_2+\epsilon_3)\boldsymbol{e}_1 + (\epsilon_4+\epsilon_5+\epsilon_6)\boldsymbol{e}_2 + \cdots + 0\epsilon_1\epsilon_2\epsilon_3\epsilon_4\epsilon_5\epsilon_6)] \quad , \tag{A.4}$$

$$\frac{\partial^2 f(\boldsymbol{x})}{\partial x_1 \partial x_2} = \epsilon_1\epsilon_4 \,\mathrm{part}\,[f(\boldsymbol{x} + (\epsilon_1+\epsilon_2+\epsilon_3)\boldsymbol{e}_1 + (\epsilon_4+\epsilon_5+\epsilon_6)\boldsymbol{e}_2 + \cdots + 0\epsilon_1\epsilon_2\epsilon_3\epsilon_4\epsilon_5\epsilon_6)] \quad , \tag{A.5}$$

$$\frac{\partial^2 f(\boldsymbol{x})}{\partial x_2^2} = \epsilon_4\epsilon_5 \,\mathrm{part}\,[f(\boldsymbol{x} + (\epsilon_1+\epsilon_2+\epsilon_3)\boldsymbol{e}_1 + (\epsilon_4+\epsilon_5+\epsilon_6)\boldsymbol{e}_2 + \cdots + 0\epsilon_1\epsilon_2\epsilon_3\epsilon_4\epsilon_5\epsilon_6)] \quad , \tag{A.6}$$

$$\frac{\partial^3 f(\boldsymbol{x})}{\partial x_1^3} = \epsilon_1\epsilon_2\epsilon_3 \,\mathrm{part}\,[f(\boldsymbol{x} + (\epsilon_1+\epsilon_2+\epsilon_3)\boldsymbol{e}_1 + (\epsilon_4+\epsilon_5+\epsilon_6)\boldsymbol{e}_2 + \cdots + 0\epsilon_1\epsilon_2\epsilon_3\epsilon_4\epsilon_5\epsilon_6)] \quad , \tag{A.7}$$

$$\frac{\partial^3 f(\boldsymbol{x})}{\partial x_1^2 \partial x_2} = \epsilon_1\epsilon_2\epsilon_4 \,\mathrm{part}[f(\boldsymbol{x} + (\epsilon_1+\epsilon_2+\epsilon_3)\boldsymbol{e}_1 + (\epsilon_4+\epsilon_5+\epsilon_6)\boldsymbol{e}_2 + \cdots + 0\epsilon_1\epsilon_2\epsilon_3\epsilon_4\epsilon_5\epsilon_6)] \quad , \tag{A.8}$$

$$\frac{\partial^3 f(\boldsymbol{x})}{\partial x_1 \partial x_2^2} = \epsilon_1\epsilon_4\epsilon_5 \,\mathrm{part}[f(\boldsymbol{x} + (\epsilon_1+\epsilon_2+\epsilon_3)\boldsymbol{e}_1 + (\epsilon_4+\epsilon_5+\epsilon_6)\boldsymbol{e}_2 + \cdots + 0\epsilon_1\epsilon_2\epsilon_3\epsilon_4\epsilon_5\epsilon_6)] \quad , \tag{A.9}$$

and

$$\frac{\partial^3 f(\boldsymbol{x})}{\partial x_2^3} = \epsilon_4\epsilon_5\epsilon_6 \,\mathrm{part}[f(\boldsymbol{x} + (\epsilon_1 + \epsilon_2 + \epsilon_3)\boldsymbol{e}_1 + (\epsilon_4 + \epsilon_5 + \epsilon_6)\boldsymbol{e}_2 + \cdots + 0\epsilon_1\epsilon_2\epsilon_3\epsilon_4\epsilon_5\epsilon_6)] \ , \tag{A.10}$$

where $\boldsymbol{e}_1 = [1, 0]$ and $\boldsymbol{e}_2 = [0, 1]$.

Steps to convert the previous real-valued code are as follows using the hypercomplex algebra library MultiZ.[22] Include the MultiZ library with `use multiz`. The MultiZ commands used in this multidual code are described in Table A.I. Convert the real-valued input vector $\boldsymbol{x}$ to a multidual vector with `type (mduvec)`. Convert the real-valued output f to a multidual number with `type (mdual)`. Include real-valued variables for the derivative values, denoted here as `d1, d2, ..., d222`. Define n for the number of nonreal parts in the multidual step, which is $2^n - 1$. For the derivative formulation in Eqs. (A.1) through (A.10), $n = 6$. Allocate the input vector with the MultiZ command `mallocate`, using n. Assign real and nonreal values to the input vector with the MultiZ interface `mset`. The nonreal components of multidual numbers, $\epsilon_1, \epsilon_2, \ldots$ are represented by `eps(1), eps(2), ...` . Evaluate the function using the MultiZ interface `mget` to retrieve specific multidual numbers from the input vector. Finally, calculate sensitivities by extracting the appropriate nonreal parts from the output, with the command `aimag`. The implementation of the multidual differentiation method in the previous real-valued code is shown on the following page.

The real part of the output is within −1.583E−14% of the original function evaluation, which is accurate to machine precision. Multidual derivative values are shown in Table A.II and compared to analytical derivatives derived using Matlab's symbolic toolbox.[26] All multidual values have machine accuracy.

TABLE A.I

MultiZ Library Functions

Function(Argument)	Description
type(mduvec)	Multidual vector type
type(mdual)	Multidual number type
mallocate(array, order, dimension)	Allocate space for multidual arrays
mset(array, column, value)	Assign value to position of multidual array
mget(array, column)	Extract value of array
eps(direction)	Unit nonreal part, ϵ_1, ϵ_2, etc.
aimag(number, [direction 1, direction 2, ...])	Extract $\epsilon_1\epsilon_2\ldots$ part from multidual number

TABLE A.II

Multidual Partial Derivative Values for $f(\boldsymbol{x}) = e^{x_2}\sin(x_1 x_2)$

Derivative	Multidual	Analytical	Difference (%)
$\partial f(\boldsymbol{x})/\partial x_1$	5.785660723519084E+01	5.785660723519084E+01	−1.583E−14
$\partial f(\boldsymbol{x})/\partial x_2$	3.295886118414182E+01	3.295886118414182E+01	3.899E−14
$\partial^2 f(\boldsymbol{x})/\partial x_1^2$	5.050989275386863E+01	5.050989275386863E+01	4.382E−14
$\partial^2 f(\boldsymbol{x})/\partial x_1 \partial x_2$	1.108154048161669E+02	1.108154048161669E+02	1.508E−13
$\partial^2 f(\boldsymbol{x})/\partial x_2^2$	9.397877389821066E+01	9.397877389821066E+01	−4.387E−14
$\partial^3 f(\boldsymbol{x})/\partial x_1^3$	−5.207094651167175E+02	−5.207094651167176E+02	3.754E−14
$\partial^3 f(\boldsymbol{x})/\partial x_1^2 \partial x_2$	−2.629564888213640E+02	−2.629564888213640E+02	−1.523E−13
$\partial^3 f(\boldsymbol{x})/\partial x_1 \partial x_2^2$	−4.520338531967883E+01	−4.520338531967884E+01	1.709E−13
$\partial^3 f(\boldsymbol{x})/\partial x_2^3$	2.316324187571217E+01	2.316324187571219E+01	1.534E−14

```
program main
use multiz           ! use MultiZ library
implicit none
! declare variables
type(mduvec) x       ! input: multidual vector
type(mdual) f        ! output: multidual number
integer n            ! size of multidual numbers for allocation
real*8 d1, d2, d11, d12, d22, d111, d112, d122, d222 ! derivatives
n = 6                ! for 6 non-real steps
! allocate multidual vector based on n and number of multidual elements
call mallocate(x, n, 2)
! assign input with non-real steps
call mset(x, 1, 2.0d0 + eps(1) + eps(2) + eps(3))
call mset(x, 2, 3.0d0 + eps(4) + eps(5) + eps(6))
! calculate output
f = exp(mget(x,2))*sin(mget(x,1)*mget(x,2))
! extract sensitivities
d1   = aimag(f,1)         ! $\partial f(\boldsymbol{x})/\partial x_1$
d2   = aimag(f,4)         ! $\partial f(\boldsymbol{x})/\partial x_2$
d11  = aimag(f,[1,2])     ! $\partial^2 f(\boldsymbol{x})/\partial x_1^2$
d12  = aimag(f,[1,4])     ! $\partial^2 f(\boldsymbol{x})/\partial x_1 \partial x_2$
d22  = aimag(f,[4,5])     ! $\partial^2 f(\boldsymbol{x})/\partial x_2^2$
d111 = aimag(f,[1,2,3])   ! $\partial^3 f(\boldsymbol{x})/\partial x_1^3$
d112 = aimag(f,[1,2,4])   ! $\partial^3 f(\boldsymbol{x})/\partial x_1^2 \partial x_2$
d122 = aimag(f,[1,4,5])   ! $\partial^3 f(\boldsymbol{x})/\partial x_1 \partial x_2^2$
d222 = aimag(f,[4,5,6])   ! $\partial^3 f(\boldsymbol{x})/\partial x_2^3$
end program
```

APPENDIX B

THIRD-ORDER MULTIDUAL-BASED DERIVATIVES OF THE UNCOLLIDED LEAKAGE

Tables B.I through B.XVI show nonzero third-order partial derivatives of the uncollided leakage with respect to material interface locations r_i, source emission rates q_i, isotope densities N_i, and microscopic cross sections σ_i for the two-region sphere described in Sec. IV. All mixed derivatives involving the source emission rate of a nuclide other than ^{239}Pu and all

TABLE B.I

Third Derivatives of L with Respect to r_i, r_j, and r_k

Surface			$\partial^3 L/\partial r_i \partial r_j \partial r_k$ (/cm^3 · s)		
i	j	k	Multidual	Central Difference	Difference (%)
r_1	r_1	r_1	4.251751234103791E+03	4.251752215506946E+03	2.308E−05
		r_2	−1.992315139941725E+03	−1.992318260969077E+03	−1.567E−04
r_2	r_2	r_1	5.788609115441809E+02	5.788627857913631E+02	3.238E−04
		r_2	−1.511995478546646E+02	−1.511998538513937E+02	−2.024E−04

TABLE B.II

Third Derivatives of L with Respect to r_i, r_j and q_k

Surface		Isotope	$\partial^3 L/\partial r_i \partial r_j \partial q_k$ [(10^{24} atoms)/cm^2 · γ]		
i	j	k	Multidual	Central Difference	Difference (%)
r_1	r_1	^{239}Pu	1.295503671170679E−01	1.295504190585887	4.009E−05
r_1	r_2	^{239}Pu	−3.192314575353601E−02	−3.192317297671331	−8.528E−05
r_2	r_2	^{239}Pu	5.410239316916306E−03	5.410250271709713	2.025E−04

TABLE B.III

Third Derivatives of L with Respect to r_i, r_j, and N_k

Surface		Isotope	$\partial^3 L/\partial r_i \partial r_j \partial N_k$ (b/atom · cm · s)		
i	j	k	Multidual	Central Difference	Difference (%)
r_1	r_1	^{239}Pu	2.299329175365145E+04	2.299330830379652E+04	7.198E−05
		^{240}Pu	−3.521000224462152E+05	−3.521002723659466E+05	−7.098E−05
		^{69}Ga	−5.458407469809417E+04	−5.458411344168442E+04	−7.098E−05
		^{71}Ga	−5.458407469809417E+04	−5.458411344168442E+04	−7.098E−05
		C	1.781351136108845E+04	1.781374796668144E+04	1.328E−03
		^{1}H	2.969140054221760E+03	2.969179491259725E+03	1.328E−03
r_1	r_2	^{239}Pu	−5.778472385972107E+03	−5.778477781742709E+03	−9.338E−05
		^{240}Pu	8.665012358673374E+04	8.665019701358714E+04	8.474E−05
		^{69}Ga	1.343287849173557E+04	1.343288987413044E+04	8.474E−05
		^{71}Ga	1.343287849173557E+04	1.343288987413044E+04	8.474E−05
		C	−5.789493720415803E+04	−5.789502675147173E+04	−1.547E−04
		^{1}H	−9.649876069072539E+03	−9.649890994776022E+03	−1.547E−04
r_2	r_2	^{239}Pu	1.131198893309447E+03	1.131200888904411E+03	8.821E−05
		^{240}Pu	−1.453332326248464E+04	−1.453334471574758E+04	−7.381E−05
		^{69}Ga	−2.253018892358022E+03	−2.253022218237153E+03	−7.381E−05
		^{71}Ga	−2.253018892358022E+03	−2.253022218237153E+03	−7.381E−05
		C	1.907804614095699E+04	1.907806928004714E+04	6.064E−05
		^{1}H	3.179911574151605E+03	3.179915430961244E+03	6.064E−05

TABLE B.IV

Third Derivatives of L with Respect to r_i, r_j, and σ_k

Surface		Isotope	$\partial^3 L/\partial r_i \partial r_j \partial \sigma_k$ (/b · cm^2 · s)		
i	j	k	Multidual	Central Difference	Difference (%)
r_1	r_1	^{239}Pu	−3.092906039971821E+02	−3.092908235353594E+02	−7.098E−05
		^{240}Pu	−1.950738052784761E+01	−1.950739437409566E+01	−7.098E−05
		^{69}Ga	−1.732673038572939E+00	−1.732674268426952E+00	−7.098E−05
		^{71}Ga	−1.149832173168731E+00	−1.149832989317951E+00	−7.098E−05
		C	4.680281574668018E+02	4.680343740163965E+02	1.328E−03
		^{1}H	9.360557061713768E+02	9.360681391395144E+02	1.328E−03
r_1	r_2	^{239}Pu	7.611493141743628E+01	7.611499591383802E+01	8.474E−05
		^{240}Pu	4.800672609583966E+00	4.800676677399548E+00	8.473E−05
		^{69}Ga	4.264025088231311E−01	4.264028701433664E−01	8.474E−05
		^{71}Ga	2.829681725575379E−01	2.829684123344232E−01	8.474E−05
		C	−1.521118449757602E+03	−1.521120802508967E+03	−1.547E−04
		^{1}H	−3.042234921002928E+03	−3.042239626483106E+03	−1.547E−04
r_2	r_2	^{239}Pu	−1.276631651060692E+01	−1.276633535563556E+01	−7.381E−05
		^{240}Pu	−8.051890063676819E−01	−8.051901949441699E−01	−7.381E−05
		^{69}Ga	−7.151802264261059E−02	−7.151812821604923E−02	−7.381E−05
		^{71}Ga	−4.746061234011698E−02	−4.746068239885472E−02	−7.381E−05
		C	5.012522574815453E+02	5.012528654293667E+02	6.064E−05
		^{1}H	1.002503862986418E+03	1.002505078912413E+03	6.064E−05

TABLE B.V

Third Derivatives of L with Respect to r_i, q_j, and N_k

Surface	Isotope		$\partial^3 L/\partial r_i \partial q_j \partial N_k$ [(10^{24} atoms) · b/atom · γ]		
i	j	k	Multidual	Central Difference	Difference (%)
r_1	^{239}Pu	^{239}Pu	4.399225649486382E−01	4.399226661807353E−01	2.301E−05
		^{240}Pu	−6.738321383247331E+00	−6.738322924322449E+00	−2.287E−05
		^{69}Ga	−1.044603846280985E+00	−1.044604085185120E+00	−2.287E−05
		^{71}Ga	−1.044603846280985E+00	−1.044604085185120E+00	−2.287E−05
		C	−1.543424314138348E+00	−1.543423151142312E+00	−7.535E−05
		^{1}H	−2.572565767004350E−01	−2.572563828532934E−01	−7.535E−05
r_2	^{239}Pu	^{239}Pu	−7.419957087684670E−02	−7.419958917390788E−02	−2.466E−05
		^{240}Pu	9.888123250957723E−01	9.888125413979227E−01	2.187E−05
		^{69}Ga	1.532899811833114E−01	1.532900147154001E−01	2.187E−05
		^{71}Ga	1.532899811833114E−01	1.532900147154001E−01	2.187E−05
		C	−5.564456475777930E−01	−5.564459559021367E−01	−5.541E−05
		^{1}H	−9.274786013438953E−02	−9.274791152561804E−02	−5.541E−05

derivatives higher than the first of any source emission rate are zero. Third-order multidual-based derivatives are compared to central differences using lower-order adjoint-based derivatives with Eq. (27). When second-order adjoint-based derivatives were not directly available, Eq. (26) was used to estimate the second-order derivative values in Eq. (27). Available adjoint-based sensitivities are given in Sec. IV. All indices of the variables in Tables B.I through B.XVI match the indices in Eq. (27). All central difference step sizes were 0.1% of the variable being perturbed, and all multidual step sizes were one. The multidual sensitivities are in excellent agreement with all central difference estimates.

TABLE B.VI

Third Derivatives of L with Respect r_i, q_j, and σ_k

Surface	Isotope		$\partial^3 L/\partial r_i \partial q_j \partial \sigma_k$ (10^{24} atoms/b · cm · γ)		
i	j	k	Multidual	Central Difference	Difference (%)
r_1	^{239}Pu	^{239}Pu	−5.919055261832739E−03	−5.919056615538993E−03	−2.287E−05
		^{240}Pu	−3.733228939569786E−04	−3.733229793370753E−04	−2.287E−05
		^{69}Ga	−3.315906572478455E−05	−3.315907330836530E−05	−2.287E−05
		^{71}Ga	−2.200493673865683E−05	−2.200494177125409E−05	−2.287E−05
		C	−4.055158038709645E−02	−4.055154983080128E−02	−7.535E−05
		^{1}H	−8.110310802892537E−02	−8.110304691637418E−02	−7.535E−05
r_2	^{239}Pu	^{239}Pu	8.685894398528359E−04	8.685896298563610E−04	2.187E−05
		^{240}Pu	5.478312146150311E−05	5.478313344528593E−05	2.187E−05
		^{69}Ga	4.865914077480003E−06	4.865915141896451E−06	2.187E−05
		^{71}Ga	3.229105799885528E−06	3.229106506250423E−06	2.187E−05
		C	−1.461992674477083E−02	−1.461993484561571E−02	−5.541E−05
		^{1}H	−2.923983447346534E−02	−2.923985067514340E−02	−5.541E−05

TABLE B.VII

Third Derivatives of L with Respect to r_i, N_j, and N_k

Surface	Isotope		$\partial^3 L/\partial r_i \partial N_j \partial N_k$ (b^2 · cm/atom^2 · s)		
i	j	k	Multidual	Central Difference	Difference (%)
r_1	^{239}Pu	^{239}Pu	−2.405077226812034E+06	−2.405077782247960E+06	−2.309E−05
		^{240}Pu	1.710470384159732E+07	1.710470774810237E+07	2.284E−05
		^{69}Ga	2.651645477589113E+06	2.651646083192979E+06	2.284E−05
		^{71}Ga	2.651645477589113E+06	2.651646083192979E+06	2.284E−05
		C	−2.649403270396002E+05	−2.649401193364382E+05	−7.840E−05
		^{1}H	−4.416001545378775E+04	−4.415998083397424E+04	−7.840E−05
	^{240}Pu	^{240}Pu	3.661448491000680E+07	3.661449327845859E+07	2.286E−05
		^{69}Ga	5.676136472457481E+06	5.676137769771774E+06	2.286E−05
		^{71}Ga	5.676136472457474E+06	5.676137769771774E+06	2.286E−05
		C	4.203809195558528E+06	4.203806035983306E+06	7.516E−05
		^{1}H	7.006871362882113E+05	7.006866096531330E+05	7.516E−05
	^{69}Ga	^{69}Ga	8.799393281962108E+05	8.799395293114757E+05	2.286E−05
		^{71}Ga	8.799393281962108E+05	8.799395293114757E+05	2.286E−05
		C	6.516927592129117E+05	6.516922694018099E+05	7.516E−05
		^{1}H	1.086235630473206E+05	1.086234814060598E+05	7.516E−05
	^{71}Ga	^{71}Ga	8.799393281962108E+05	8.799395293114757E+05	2.286E−05
		C	6.516927592129117E+05	6.516922694018099E+05	7.516E−05
		^{1}H	1.086235630473206E+05	1.086234814060598E+05	7.516E−05
	C	C	7.540515837099529E+05	7.540504338395152E+05	1.525E−04
		^{1}H	1.256846398646119E+05	1.256844482052651E+05	1.525E−04
	^{1}H	^{1}H	2.094900274617472E+04	2.094897080056757E+04	1.525E−04
r_2	^{239}Pu	^{239}Pu	4.276679332394132E+05	4.276680419030944E+05	2.541E−05
		^{240}Pu	−2.435287227718840E+06	−2.435287745324586E+06	−2.125E−05
		^{69}Ga	−3.775288028259811E+05	−3.775288830675392E+05	−2.125E−05
		^{71}Ga	−3.775288028259811E+05	−3.775288830675392E+05	−2.125E−05
		C	−1.094541658148352E+05	−1.094542320224671E+05	−6.049E−05

(Continued)

TABLE B.VII (Continued)

Surface	Isotope		$\partial^3 L/\partial r_i \partial N_j \partial N_k$ ($b^2 \cdot$ cm/atom$^2 \cdot$ s)		
i	j	k	Multidual	Central Difference	Difference (%)
		^{1}H	−1.824372192739881E+04	−1.824373296282079E+04	−6.049E−05
	^{240}Pu	^{240}Pu	−5.298242388677118E+06	−5.298243532553001E+06	−2.159E−05
		^{69}Ga	−8.213565460829767E+05	−8.213567234116945E+05	−2.159E−05
		^{71}Ga	−8.213565460829758E+05	−8.213567234116945E+05	−2.159E−05
		C	1.501649274235141E+06	1.501650100734221E+06	5.504E−05
		^{1}H	2.502935506170844E+05	2.502936883771510E+05	5.504E−05
	^{69}Ga	^{69}Ga	−1.273302590374299E+05	−1.273302865277079E+05	−2.159E−05
		^{71}Ga	−1.273302590374306E+05	−1.273302865277079E+05	−2.159E−05
		C	2.327921923598021E+05	2.327923204872821E+05	5.504E−05
		^{1}H	3.880159327573198E+04	3.880161463189551E+04	5.504E−05
	^{71}Ga	^{71}Ga	−1.273302590374299E+05	−1.273302865277079E+05	−2.159E−05
		C	2.327921923598021E+05	2.327923204872821E+05	5.504E−05
		^{1}H	3.880159327573198E+04	3.880161463189551E+04	5.504E−05
	C	C	1.383480814866549E+06	1.383480215788865E+06	4.330E−05
		^{1}H	2.305973380767888E+05	2.305972382230618E+05	4.330E−05
	^{1}H	^{1}H	3.843575693764147E+04	3.843574029411131E+04	4.330E−05

TABLE B.VIII

Third Derivatives of L with Respect r_i, N_j, and σ_k

Surface	Isotope		$\partial^3 L/\partial r_i \partial N_j \partial \sigma_k$ (/atom · s)		
i	j	k	Multidual	Central Difference	Difference (%)
r_1	^{239}Pu	^{239}Pu	−2.112660439418824E+03	−2.112660927329259E+03	−2.309E−05
		^{240}Pu	9.476510803266009E+02	9.476512967584690E+02	2.284E−05
		^{69}Ga	8.417170488433543E+01	8.417172410811681E+01	2.284E−05
		^{71}Ga	5.585781748308673E+01	5.585783024031718E+01	2.284E−05
		C	−6.960982065212679E+03	−6.960976608099394E+03	−7.840E−05
		^{1}H	−1.392195507630569E+04	−1.392194416213061E+04	−7.840E−05
	^{240}Pu	^{239}Pu	3.216278168397899E+04	3.216278903496936E+04	2.286E−05
		^{240}Pu	−1.510917052367745E+04	−1.510917397949045E+04	−2.287E−05
		^{69}Ga	1.801787184904126E+02	1.801787596712963E+02	2.286E−05
		^{71}Ga	1.195697531088852E+02	1.195697804372360E+02	2.286E−05
		C	1.104499293966844E+05	1.104498463827122E+05	7.516E-05
		^{1}H	2.208997151316169E+05	2.208995491037624E+05	7.516E−05
	^{69}Ga	^{239}Pu	4.986014104003578E+03	4.986015243586005E+03	2.286E−05
		^{240}Pu	3.144747146761016E+02	3.144747865511128E+02	2.286E−05
		^{69}Ga	−1.710978897421775E+04	−1.710979288728414E+04	−2.287E−05
		^{71}Ga	1.853622243470614E+01	1.853622667126557E+01	2.286E−05
		C	1.712242775420094E+04	1.712241488501462E+04	7.516E−05
		^{1}H	3.424483323733318E+04	3.424480749897502E+04	7.516E−05
	^{71}Ga	^{239}Pu	4.986014104003578E+03	4.986015243586005E+03	2.286E−05
		^{240}Pu	3.144747146761016E+02	3.144747865511128E+02	2.286E−05
		^{69}Ga	2.793208748116422E+01	2.793209386520320E+01	2.286E−05
		^{71}Ga	−1.711918483926420E+04	−1.711918875447780E+04	−2.287E−05

(Continued)

TABLE B.VIII (Continued)

Surface	Isotope		$\partial^3 L/\partial r_i \partial N_j \partial \sigma_k$ (/atom · s)		
i	j	k	Multidual	Central Difference	Difference (%)
r_2	C	C	1.712242775420094E+04	1.712241488501462E+04	7.516E−05
		^{1}H	3.424483323733318E+04	3.424480749897502E+04	7.516E−05
		^{239}Pu	3.692696967611851E+03	3.692694192187203E+03	7.516E−05
		^{240}Pu	2.329034377064027E+02	2.329032626565962E+02	7.516E−05
		^{69}Ga	2.068681166744851E+01	2.068679611927638E+01	7.516E−05
		^{71}Ga	1.372813051624873E+01	1.372812019821084E+01	7.516E−05
	^{1}H	C	−1.135170772560420E+05	−1.135170070019562E+05	−6.189E−05
		^{1}H	3.962353481981540E+04	3.962347439698634E+04	1.525E−04
		^{239}Pu	6.154954097702189E+02	6.154949471649068E+02	7.516E−05
		^{240}Pu	3.882013555006197E+01	3.882010637291675E+01	7.516E−05
		^{69}Ga	3.448059165366621E+00	3.448056573811286E+00	7.516E−05
		^{71}Ga	2.288192448930383E+00	2.288190729129234E+00	7.516E−05
	^{239}Pu	C	3.302209723019966E+03	3.302204687404855E+03	1.525E−04
		^{1}H	−1.267244423996289E+05	−1.267243520053234E+05	−7.133E−05
		^{239}Pu	3.756707326028520E+02	3.756708280522187E+02	2.541E−05
		^{240}Pu	−1.349221005885489E+02	−1.349221292654508E+02	−2.125E−05
		^{69}Ga	−1.198397117766172E+01	−1.198397372479148E+01	−2.125E−05
		^{71}Ga	−7.952773152026001E+00	−7.952774842338610E+00	−2.125E−05
	^{240}Pu	C	−2.875773928843979E+03	−2.875775668369204E+03	−6.049E−05
		^{1}H	−5.751544117181082E+03	−5.751547596214911E+03	−6.049E−05
		^{239}Pu	−4.654065561065781E+03	−4.654066565868075E+03	−2.159E−05
		^{240}Pu	2.221329879819625E+03	2.221330366571009E+03	2.191E−05
		^{69}Ga	−2.607248268519335E+01	−2.607248831417609E+01	−2.159E−05
		^{71}Ga	−1.730215612433793E+01	−1.730215985982624E+01	−2.159E−05
	^{69}Ga	C	3.945399246309453E+04	3.945401417833659E+04	5.504E−05
		^{1}H	7.890793360854947E+04	7.890797703901881E+04	5.504E−05
		^{239}Pu	−7.214934565187295E+02	−7.214936122876146E+02	−2.159E−05
		^{240}Pu	−4.550557702939847E+01	−4.550558685392662E+01	−2.159E−05
		^{69}Ga	2.510826277332108E+03	2.510826826585147E+03	2.188E−05
		^{71}Ga	−2.682255388021778E+00	−2.682255967113402E+00	−2.159E−05
	^{71}Ga	C	6.116329265706205E+03	6.116332632097205E+03	5.504E−05
		^{1}H	1.223265057592904E+04	1.223265730870981E+04	5.504E−05
		^{239}Pu	−7.214934565187295E+02	−7.214936122876146E+02	−2.159E−05
		^{240}Pu	−4.550557702939847E+01	−4.550558685392662E+01	−2.159E−05
		^{69}Ga	−4.041869502211551E+00	−4.041870374840511E+00	−2.159E−05
		^{71}Ga	2.512185891446298E+03	2.512186440992889E+03	2.188E−05
	C	C	6.116329265706205E+03	6.116332632097205E+03	5.504E−05
		^{1}H	1.223265057592904E+04	1.223265730870981E+04	5.504E−05
		^{239}Pu	1.319074073876443E+03	1.319074799886742E+03	5.504E−05
		^{240}Pu	8.319580217108823E+01	8.319584796156407E+01	5.504E−05
		^{69}Ga	7.389568432240856E+00	7.389572499415835E+00	5.504E−05
		^{71}Ga	4.903847027146357E+00	4.903849726194565E+00	5.504E−05
	^{1}H	C	−1.171934952477799E+04	−1.171939189944461E+04	−3.616E−04
		^{1}H	7.269847504424478E+04	7.269844356420336E+04	4.330E−05
		^{239}Pu	2.198620804086495E+02	2.198622014193878E+02	5.504E−05
		^{240}Pu	1.386700148904244E+01	1.386700912135836E+01	5.504E−05
		^{69}Ga	1.231686620949188E+00	1.231687298862262E+00	5.504E−05
		^{71}Ga	8.173688125229283E−01	8.173692623978777E−01	5.504E−05
		C	6.058662162058663E+03	6.058659538524116E+03	4.330E−05
		^{1}H	−3.595129424292349E+04	−3.595132612462629E+04	−8.868E−05

TABLE B.IX

Third Derivatives of L with Respect to r_i, σ_j, and σ_k

Surface	Isotope		$\partial^3 L/\partial r_i \partial\sigma_j \partial\sigma_k$ (/b^2 · cm · s)		
i	j	k	Multidual	Central Difference	Difference (%)
r_1	^{239}Pu	^{239}Pu	2.825233041496587E+01	2.825233687220014E+01	2.286E−05
		^{240}Pu	1.781913039324802E+00	1.781913446591256E+00	2.286E−05
		^{69}Ga	1.582720281645272E−01	1.582720643385066E−01	2.286E−05
		^{71}Ga	1.050320897508326E−01	1.050321137565182E−01	2.286E−05
		C	9.702108263786015E+01	9.702100971699156E+01	7.516E−05
		^{1}H	1.940420390808121E+02	1.940418932391511E+02	7.516E−05
	^{240}Pu	^{240}Pu	1.123876874253803E−01	1.123877131122354E−01	2.286E−05
		^{69}Ga	9.982432833128597E−03	9.982435114670719E−03	2.286E−05
		^{71}Ga	6.624517253111261E−03	6.624518767182508E−03	2.286E−05
		C	6.119252100712798E+00	6.119247501493735E+00	7.516E−05
		^{1}H	1.223849624214051E+01	1.223848704370789E+01	7.516E−05
	^{69}Ga	^{69}Ga	8.866537567479147E−04	8.866539593977185E−04	2.286E−05
		^{71}Ga	5.883989611850573E−04	5.883990956670131E−04	2.286E−05
		C	5.435205980628787E−01	5.435201895537757E−01	7.516E−05
		^{1}H	1.087040489170835E+00	1.087039672153113E+00	7.516E−05
	^{71}Ga	^{71}Ga	3.904718554326126E−04	3.904719446771915E−04	2.286E−05
		C	3.606897876978187E−01	3.606895166040242E−01	7.516E−05
		^{1}H	7.213791062479700E−01	7.213785640606895E−01	7.516E−05
	C	C	5.205302222225723E+02	5.205294284541171E+02	1.525E−04
		^{1}H	1.041059767393706E+03	1.041058179857988E+03	1.525E−04
	^{1}H	^{1}H	2.082118180685416E+03	2.082115005615964E+03	1.525E−04
r_2	^{239}Pu	^{239}Pu	−4.088209760464879E+00	−4.088210643100506E+00	−2.159E−05
		^{240}Pu	−2.578489693653151E−01	−2.578490250341868E−01	−2.159E−05
		^{69}Ga	−2.290250895579349E−02	−2.290251390038664E−02	−2.159E−05
		^{71}Ga	−1.519850604090056E−02	−1.519850932221535E−02	−2.159E−05
		C	3.465705305620877E+01	3.465707213124453E+01	5.504E−05
		^{1}H	6.931406103413656E+01	6.931409918419270E+01	5.504E−05
	^{240}Pu	^{240}Pu	−1.626288642175609E−02	−1.626288993286968E−02	−2.159E−05
		^{69}Ga	−1.444492498217540E−03	−1.444492810079643E−03	−2.159E−05
		^{71}Ga	−9.585905196051120E−04	−9.585907265623055E−04	−2.159E−05
		C	2.185867637761891E+00	2.185868840850406E+00	5.504E−05
		^{1}H	4.371732432375074E+00	4.371734838551284E+00	5.504E−05
	^{69}Ga	^{69}Ga	−1.283018600323861E−04	−1.283018877324248E−04	−2.159E−05
		^{71}Ga	−8.514336130268046E−05	−8.514337968490349E−05	−2.159E−05
		C	1.941518450635893E−01	1.941519519236050E−01	5.504E−05
		^{1}H	3.883034375947023E−01	3.883036513146602E−01	5.504E−05
	^{71}Ga	^{71}Ga	−5.650262569918219E−05	−5.650263789794492E−05	−2.159E−05
		C	1.288425646179915E−01	1.288426355321758E−01	5.504E−05
		^{1}H	2.576849616510092E−01	2.576851034793252E−01	5.504E−05
	C	C	9.550322438950732E+02	9.550318303450093E+02	4.330E−05
		^{1}H	1.910063245583783E+03	1.910062418484297E+03	4.330E−05
	^{1}H	^{1}H	3.820124006756455E+03	3.820122352558588E+03	4.330E−05

TABLE B.X

Third Derivatives of L with Respect to q_i, N_j, and N_k

Isotope			$\partial^3 L/\partial q_i \partial N_j \partial N_k$ [(10^{24} atoms) · b^2 · $cm^2/atom^2$ · γ]		
i	j	k	Multidual	Central Difference	Difference (%)
^{239}Pu	^{239}Pu	^{239}Pu	−3.492366709188465E+01	−3.492366709197072E+01	−2.464E−10
		^{240}Pu	2.018281335582254E+02	2.018281335582002E+02	1.249E−11
		^{69}Ga	3.128827383134277E+01	3.128827383133877E+01	1.279E−11
		^{71}Ga	3.128827383134270E+01	3.128827383132661E+01	5.143E−11
		C	−5.978929529880229E+00	−5.978929529836059E+00	−7.388E−10
		^{1}H	−9.965625972717803E−01	−9.965625972621418E−01	−9.672E−10
	^{240}Pu	^{240}Pu	4.385799342083405E+02	4.385799342083296E+02	2.488E−12
		^{69}Ga	6.799056621352570E+01	6.799056621351731E+01	1.233E−11
		^{71}Ga	6.799056621352564E+01	6.799056621351731E+01	1.225E−11
		C	7.707204346879145E+01	7.707204346873539E+01	7.274E−11
		^{1}H	1.284629889554514E+01	1.284629889554935E+01	3.277E−11
	^{69}Ga	^{69}Ga	1.054019286673501E+01	1.054019286673419E+01	7.786E−12
		^{71}Ga	1.054019286673493E+01	1.054019286673419E+01	7.028E−12
		C	1.194804291293285E+01	1.194804291293392E+01	8.950E−12
		^{1}H	1.991489048017869E+00	1.991489048018332E+00	2.325E−11
	^{71}Ga	^{71}Ga	1.054019286673501E+01	1.054019286673149E+01	3.340E−11
		C	1.194804291293290E+01	1.194804291293392E+01	8.534E−12
		^{1}H	1.991489048017869E+00	1.991489048018332E+00	2.325E−11
	C	C	2.757030935587084E+01	2.757030935585430E+01	6.000E−11
		^{1}H	4.595394369838559E+00	4.595394369835828E+00	5.941E−11
	^{1}H	^{1}H	7.659562009900740E−01	7.659562009895743E−01	6.524E−11

TABLE B.XI

Third Derivatives of L with Respect to q_i, N_j, and σ_k

Isotope			$\partial^3 L/\partial q_i \partial N_j \partial \sigma_k$ [(10^{24} atoms) · cm/atom · γ]		
i	j	k	Multidual	Central Difference	Difference (%)
^{239}Pu	^{239}Pu	^{239}Pu	−3.067753876754492E−02	−3.067753876760657E−02	−2.010E−10
		^{240}Pu	1.118187432989147E−02	1.118187432988489E−02	5.884E−11
		^{69}Ga	9.931898413759782E−04	9.931898413755920E−04	3.888E−11
		^{71}Ga	6.590981727395154E−04	6.590981727391025E−04	6.264E−11
		C	−1.570890384703374E−01	−1.570890384689679E−01	−8.718E−10
		^{1}H	−3.141778726156328E−01	−3.141778726116834E−01	−1.257E−09
	^{240}Pu	^{239}Pu	3.852560184743039E−01	3.852560184743800E−01	1.975E−11
		^{240}Pu	−1.836681557209859E−01	−1.836681557210812E−01	−5.188E−11
		^{69}Ga	2.158237940407871E−03	2.158237940407621E−03	1.157E−11
		^{71}Ga	1.432244495059661E−03	1.432244495059357E−03	2.123E−11
		C	2.024973390460598E+00	2.024973390461067E+00	2.316E−11
		^{1}H	4.049944147046950E+00	4.049944147048918E+00	4.860E−11
	^{69}Ga	^{239}Pu	5.972406120338720E−02	5.972406120339742E−02	1.711E−11
		^{240}Pu	3.766878054186054E−03	3.766878054185416E−03	1.694E−11
		^{69}Ga	−2.076321992018803E−01	−2.076321992019677E−01	−4.209E−11
		^{71}Ga	2.220327620575847E−04	2.220327620575310E−04	2.418E−11
		C	3.139201697251767E−01	3.139201697252462E−01	2.214E−11

(Continued)

TABLE B.XI (Continued)

Isotope			$\partial^3 L/\partial q_i \partial N_j \partial \sigma_k$ [(10^{24} atoms) · cm/atom · γ]		
i	j	k	Multidual	Central Difference	Difference (%)
		^{1}H	6.278399311357282E−01	6.278399311360133E−01	4.541E−11
	^{71}Ga	^{239}Pu	5.972406120338720E−02	5.972406120339742E−02	1.711E−11
		^{240}Pu	3.766878054186054E−03	3.766878054185416E−03	1.694E−11
		^{69}Ga	3.345794190441425E−04	3.345794190441288E−04	4.083E−12
		^{71}Ga	−2.077447458588668E−01	−2.077447458589609E−01	−4.531E−11
		C	3.139201697251767E−01	3.139201697252462E−01	2.214E−11
		^{1}H	6.278399311357282E−01	6.278399311360133E−01	4.541E−11
	C	^{239}Pu	6.770138414115646E−02	6.770138414117033E−02	2.048E−11
		^{240}Pu	4.270018699680769E−03	4.270018699682470E−03	3.985E−11
		^{69}Ga	3.792690804681544E−04	3.792690804682470E−04	2.441E−11
		^{71}Ga	2.516896040406913E−04	2.516896040407694E−04	3.104E−11
		C	−1.753518777003890E+00	−1.753518777003498E+00	−2.236E−11
		^{1}H	1.448751168163630E+00	1.448751168162683E+00	6.537E−11
	^{1}H	^{239}Pu	1.128440582572930E−02	1.128440582573177E−02	2.189E−11
		^{240}Pu	7.117228768940148E−04	7.117228768942675E−04	3.551E−11
		^{69}Ga	6.321622926099207E−05	6.321622926101034E−05	2.890E−11
		^{71}Ga	4.195139686052158E−05	4.195139686053661E−05	3.583E−11
		C	1.207383494557380E−01	1.207383494556542E−01	6.940E−11
		^{1}H	−2.236418290314506E+00	−2.236418290313802E+00	−3.147E−11

TABLE B.XII

Third Derivatives of L with Respect to q_i, σ_j, and σ_k

Isotope			$\partial^3 L/\partial q_i \partial \sigma_j \partial \sigma_k$ (10^{24} atoms/b^2 · γ)		
i	j	k	Multidual	Central Difference	Difference (%)
^{239}Pu	^{239}Pu	^{239}Pu	3.384153906598177E−04	3.384153906598862E−04	2.025E−11
		^{240}Pu	2.134432057348066E−05	2.134432057347827E−05	1.121E−11
		^{69}Ga	1.895832643010848E−06	1.895832643010672E−06	9.282E−12
		^{71}Ga	1.258107744132024E−06	1.258107744131729E−06	2.345E−11
		C	1.778770812516648E−03	1.778770812517101E−03	2.547E−11
		^{1}H	3.557539311393691E−03	3.557539311395360E−03	4.692E−11
	^{240}Pu	^{240}Pu	1.346215430259401E−06	1.346215430259250E−06	1.122E−11
		^{69}Ga	1.195727523124645E−07	1.195727523124530E−07	9.630E−12
		^{71}Ga	7.935057254451509E−08	7.935057254449236E−08	2.865E−11
		C	1.121895028919376E−04	1.121895028919617E−04	2.148E−11
		^{1}H	2.243788598594675E−04	2.243788598595870E−04	5.326E−11
	^{69}Ga	^{69}Ga	1.062062042538242E−08	1.062062042538214E−08	2.632E−12
		^{71}Ga	7.048029716082934E−09	7.048029716081643E−09	1.832E−11
		C	9.964829803481977E−06	9.964829803483791E−06	1.821E−11
		^{1}H	1.992964664575235E−05	1.992964664576202E−05	4.852E−11
	^{71}Ga	^{71}Ga	4.677195953643981E−09	4.677195953642914E−09	2.281E−11
		C	6.612835574351154E−06	6.612835574352860E−06	2.580E−11
		^{1}H	1.322566254741530E−05	1.322566254742131E−05	4.545E−11
	C	C	1.903209218810780E−02	1.903209218809492E−02	6.769E−11
		^{1}H	3.806415962125451E−02	3.806415962123275E−02	5.717E−11
	^{1}H	^{1}H	7.612826973261906E−02	7.612826973257168E−02	6.224E−11

TABLE B.XIII

Third Derivatives of L with Respect to N_i, N_j, and N_k

Isotope			$\partial^3 L/\partial N_i \partial N_j \partial N_k$ ($b^3 \cdot cm^3/atom^3 \cdot s$)		
i	j	k	Multidual	Central Difference	Difference (%)
^{239}Pu	^{239}Pu	^{239}Pu	2.995730212289502E+08	2.9957398197353202E+08	3.207E−04
		^{240}Pu	−9.702682360721366E+08	−9.7026941897914159E+08	−1.219E−04
		^{69}Ga	−1.504151959633565E+08	−1.5041537934273025E+08	−1.219E−04
		^{71}Ga	−1.504151959633616E+08	−1.5041537934273025E+08	−1.219E−04
		C	3.465300288351038E+07	3.4653070327737480E+07	1.946E−04
		^{1}H	5.775931357657159E+06	5.7759425992011903E+06	1.946E−04
	^{240}Pu	^{240}Pu	−2.240109493373314E+09	−2.2401128199320970E+09	−1.485E−04
		^{69}Ga	−3.472715027641820E+08	−3.4727201846179771E+08	−1.485E−04
		^{71}Ga	−3.472715027641796E+08	−3.4727201846179771E+08	−1.485E−04
		C	−1.884973351677643E+08	−1.8849745639059082E+08	−6.431E−05
		^{1}H	−3.141856631271924E+07	−3.1418586516403344E+07	−6.431E−05
	^{69}Ga	^{69}Ga	−5.383553660606406E+07	−5.3835616551742688E+07	−1.485E−04
		^{71}Ga	−5.383553660606465E+07	−5.3835616530151561E+07	−1.485E−04
		C	−2.922167556737571E+07	−2.9221694358354200E+07	−6.431E−05
		^{1}H	−4.870642604921388E+06	−4.8706457369847512E+06	−6.431E−05
	^{71}Ga	^{71}Ga	−5.383553660606465E+07	−5.3835832461315297E+07	−5.496E−04
		C	−2.922167556737587E+07	−2.9221694336763080E+07	−6.423E−05
		^{1}H	−4.870642604921388E+06	−4.8706457369847512E+06	−6.436E−05
	C	C	6.029473460001338E+06	6.0294794948277874E+06	1.001E−04
		^{1}H	1.004987214090909E+06	1.0049882199687074E+06	1.001E−04
	^{1}H	^{1}H	1.675103650735670E+05	1.6751053273251091E+05	1.001E−04
^{240}Pu	^{240}Pu	^{240}Pu	−3.509950750674471E+09	−3.5099507894888191E+09	1.106E−06
		^{69}Ga	−5.441278095649949E+08	−5.4412781558207130E+08	−1.106E−06
		^{71}Ga	−5.441278095650114E+08	−5.4412781558207130E+08	−1.106E−06
		C	−4.116476732190798E+08	−4.1164767595187926E+08	−6.639E−07
		^{1}H	−6.861306398309547E+07	−6.8613064438843742E+07	−6.642E−07
	^{69}Ga	^{69}Ga	−8.435305626014875E+07	−8.4353057192841396E+07	−1.106E−06
		^{71}Ga	−8.435305626015280E+07	−8.4353057192841396E+07	−1.106E−06
		C	−6.381541014447919E+07	−6.3815410568303041E+07	−6.641E−07
		^{1}H	−1.063669517456582E+07	−1.0636695245218094E+07	−6.642E−07
	^{71}Ga	^{71}Ga	−8.435305626015291E+07	−8.4353057192841396E+07	−1.106E−06
		C	−6.381541014447957E+07	−6.3815410568303041E+07	−6.641E−07
		^{1}H	−1.063669517456588E+07	−1.0636695245218094E+07	−6.642E−07
	C	C	−7.379614911399059E+07	−7.3796149359120727E+07	−3.322E−07
		^{1}H	−1.230027577046341E+07	−1.2300275811329843E+07	−3.322E−07
	^{1}H	^{1}H	−2.050198903952919E+06	−2.0501989107833165E+06	−3.332E−07
^{69}Ga	^{69}Ga	^{69}Ga	−1.307677713829100E+07	−1.3076777137744062E+07	4.183E−09
		^{71}Ga	−1.307677713829186E+07	−1.3076777137744062E+07	−4.189E−09
		C	−9.892942039638313E+06	−9.892942041141208E+06	−1.519E−08
		^{1}H	−1.648946682580927E+06	−1.648946682826353E+06	−1.488E−08
	^{71}Ga	^{71}Ga	−1.307677713829100E+07	−1.307677713774406E+07	−4.183E−09
		C	−9.892942039638393E+06	−9.892942041141208E+06	−1.519E−08
		^{1}H	−1.648946682580939E+06	−1.648946682826353E+06	−1.488E−08
	C	C	−1.144019954240438E+07	−1.144019954454673E+07	−1.873E−08
		^{1}H	−1.906842171714688E+06	−1.906842172029414E+06	−1.651E−08
	^{1}H	^{1}H	−3.178307383846062E+05	−3.178307383469324E+05	−1.185E−08
^{71}Ga	^{71}Ga	^{71}Ga	−1.307677713829178E+07	−1.307677713722310E+07	8.172E−09

(Continued)

TABLE B.XIII (Continued)

Isotope			$\partial^3 L/\partial N_i \partial N_j \partial N_k$ ($b^3 \cdot cm^3/atom^3 \cdot s$)		
i	j	k	Multidual	Central Difference	Difference (%)
		C	−9.892942039638313E+06	−9.892942039418800E+06	−2.219E−09
		^{1}H	−1.648946682580927E+06	−1.648946682586822E+06	−3.575E−10
	C	C	−1.144019954240438E+07	−1.144019953725010E+07	−4.505E−08
		^{1}H	−1.906842171714688E+06	−1.906842170800369E+06	−4.795E−08
	^{1}H	^{1}H	−3.178307383846062E+05	−3.178307381680259E+05	−6.814E−08
C	C	C	−2.696827683306663E+07	−2.696827725347538E+07	1.559E−06
		^{1}H	−4.495048130337075E+06	−4.49504820040948E+06	−1.559E−06
	^{1}H	^{1}H	−7.492305800299522E+05	−7.492305917101883E+05	−1.559E−06
^{1}H	^{1}H	^{1}H	−1.248810793066914E+05	−1.248810795228643E+05	1.731E−07

TABLE B.XIV

Third Derivatives of L with Respect to N_i, N_j, and σ_k

Isotope			$\partial^3 L/\partial N_i \partial N_j \partial \sigma_k$ ($b \cdot cm^2/atom^2 \cdot s$)		
i	j	k	Multidual	Central Difference	Difference (%)
^{239}Pu	^{239}Pu	^{239}Pu	1.743278682813930E+05	1.743281948662195E+05	1.873E−04
		^{240}Pu	−5.375572419349610E+04	−5.375578973003904E+04	−1.219E−04
		^{69}Ga	−4.774659203785505E+03	−4.774665024834193E+03	−1.219E−04
		^{71}Ga	−3.168547467530565E+03	−3.168551330481496E+03	−1.219E−04
		C	9.104651385968036E+05	9.104669106140363E+05	1.946E−04
		^{1}H	1.820929092955487E+06	1.820932636987726E+06	1.946E−04
	^{240}Pu	^{239}Pu	−8.522999989864256E+05	−8.523003552364936E+05	−4.180E−05
		^{240}Pu	3.892052556290618E+05	3.892054127453684E+05	4.037E−05
		^{69}Ga	−1.102350773979886E+04	−1.102352410968920E+04	−1.485E−04
		^{71}Ga	−7.315392793804171E+03	−7.315403657150883E+03	−1.485E−04
		C	−4.952536233742326E+06	−4.952539418467350E+06	−6.430E−05
		^{1}H	−9.905066025741907E+06	−9.905072395185854E+06	−6.430E−05
	^{69}Ga	^{239}Pu	−1.321272474981654E+05	−1.321273027255915E+05	−4.180E−05
		^{240}Pu	−1.923986628524890E+04	−1.923989485641740E+04	−1.485E−04
		^{69}Ga	5.116050215874860E+05	5.116053604672791E+05	6.624E−05
		^{71}Ga	−1.134063962645450E+03	−1.134065646728607E+03	−1.485E−04
		C	−7.677636764959395E+05	−7.677641702057245E+05	−6.430E−05
		^{1}H	−1.535526354364942E+06	−1.535527341784056E+06	−6.430E−05
	^{71}Ga	^{239}Pu	−1.321272474981654E+05	−1.321273027255915E+05	−4.180E−05
		^{240}Pu	−1.923986628524890E+04	−1.923989485641740E+04	−1.485E−04
		^{69}Ga	−1.708912046423156E+03	−1.708914584154689E+03	−1.485E−04
		^{71}Ga	5.121798696712636E+05	5.121802094046901E+05	6.633E−05
		C	−7.677636764959395E+05	−7.677641702057245E+05	−6.430E−05
		^{1}H	−1.535526354364942E+06	−1.535527341784056E+06	−6.430E−05
	C	^{239}Pu	3.043978275746765E+04	3.043981184273126E+04	9.555E−05
		^{240}Pu	−1.044330875089480E+04	−1.044331546645829E+04	−6.430E−05
		^{69}Ga	−9.275894054733330E+02	−9.275900019590727E+02	−6.430E−05
		^{71}Ga	−6.155645745963376E+02	−6.155649704347742E+02	−6.430E−05

(Continued)

TABLE B.XIV (Continued)

Isotope			$\partial^3 L/\partial N_i \partial N_j \partial \sigma_k$ (b · cm^2/atom^2 · s)		
i	j	k	Multidual	Central Difference	Difference (%)
		C	−3.580733832078601E+05	−3.580737368268060E+05	−9.876E−05
		^{1}H	3.168338304020197E+05	3.168341475170545E+05	1.001E−04
	^{1}H	^{239}Pu	5.073675615938963E+03	5.073680463847417E+03	9.555E−05
		^{240}Pu	−1.740681311075983E+03	−1.740682430420075E+03	−6.430E−05
		^{69}Ga	−1.546097679359685E+02	−1.546098673576758E+02	−6.430E−05
		^{71}Ga	−1.026017497250069E+02	−1.026018157030030E+02	−6.430E−05
		C	2.640480613587222E+04	2.640483256402007E+04	1.001E−04
		^{1}H	−4.636808235079139E+05	−4.636812828277020E+05	−9.906E−05
^{240}Pu	^{240}Pu	^{239}Pu	−3.083199995655494E+06	−3.083200029755863E+06	−1.106E−06
		^{240}Pu	2.036438364852869E+06	2.036438392664305E+06	1.366E−06
		^{69}Ga	−1.727235627581222E+04	−1.727235646681950E+04	−1.106E−06
		^{71}Ga	−1.146223812007777E+04	−1.146223824681642E+04	−1.106E−06
		C	−1.081553760608144E+07	−1.081553767791507E+07	−6.642E−07
		^{1}H	−2.163106114443928E+07	−2.163106128806427E+07	−6.640E−07
	^{69}Ga	^{239}Pu	−4.779710540851522E+05	−4.779710593715602E+05	−1.106E−06
		^{240}Pu	1.427756165559226E+05	1.427756197062078E+05	2.206E−06
		^{69}Ga	1.112772362648456E+06	1.112772370109456E+06	6.705E−07
		^{71}Ga	−1.776925935439949E+03	−1.776925955087419E+03	−1.106E−06
		C	−1.676671613051589E+06	−1.676671624187005E+06	−6.641E−07
		^{1}H	−3.353341045263569E+06	−3.353341067532156E+06	−6.641E−07
^{240}Pu	^{71}Ga	^{239}Pu	−4.779710540851522E+05	−4.779710593715602E+05	−1.106E−06
		^{240}Pu	1.427756165559226E+05	1.427756197062078E+05	2.206E−06
		^{69}Ga	−2.677635686078510E+03	−2.677635715688568E+03	−1.106E−06
		^{71}Ga	1.113673072399094E+06	1.113673079870213E+06	6.709E−07
		C	−1.676671613051589E+06	−1.676671624187005E+06	−6.641E−07
		^{1}H	−3.353341045263569E+06	−3.353341067532156E+06	−6.641E−07
	C	^{239}Pu	−3.615982657411079E+05	−3.615982681423834E+05	−6.641E−07
		^{240}Pu	1.732125281033983E+05	1.732125299296868E+05	1.054E−06
		^{69}Ga	−2.025705138621213E+03	−2.025705152074431E+03	−6.641E−07
		^{71}Ga	−1.344293406711219E+03	−1.344293415639237E+03	−6.641E−07
		C	4.718972589064276E+06	4.718972605005500E+06	3.378E−07
		^{1}H	−3.877804048364988E+06	−3.877804061255515E+06	−3.324E−07
	^{1}H	^{239}Pu	−6.027087375340729E+04	−6.027087415369548E+04	−6.641E−07
		^{240}Pu	2.887090841664290E+04	2.887090872104760E+04	1.054E−06
		^{69}Ga	−3.376427108167617E+02	−3.376427130591083E+02	−6.641E−07
		^{71}Ga	−2.240656161261526E+02	−2.240656176143252E+02	−6.642E−07
		C	−3.231746559389047E+05	−3.231746570138796E+05	−3.326E−07
		^{1}H	6.011526982682471E+06	6.011527002917835E+06	3.366E−07
^{69}Ga	^{69}Ga	^{239}Pu	−7.409714869784210E+04	−7.409714869773823E+04	−1.402E−10
		^{240}Pu	−4.673408299498435E+03	−4.673408299908193E+03	−8.768E−09
		^{69}Ga	3.454287078735932E+05	3.454287078745845E+05	2.870E−10
		^{71}Ga	−2.754667759439039E+02	−2.754667759839371E+02	−1.453E−08
		C	−2.599249154690470E+05	−2.599249154595520E+05	−3.653E−09
		^{1}H	−5.198494928548661E+05	−5.198494928703172E+05	−2.972E−09
	^{71}Ga	^{239}Pu	−7.409714869784210E+04	−7.409714869773823E+04	−1.402E−10
		^{240}Pu	−4.673408299498435E+03	−4.673408299908193E+03	−8.768E−09
		^{69}Ga	1.725068045801000E+05	1.725068045807559E+05	3.802E−10
		^{71}Ga	1.726464365175494E+05	1.726464365218976E+05	2.519E−09

(Continued)

TABLE B.XIV (Continued)

Isotope			$\partial^3 L/\partial N_i \partial N_j \partial \sigma_k$ (b · cm^2/atom^2 · s)		
i	*j*	*k*	Multidual	Central Difference	Difference (%)
		C	−2.599249154690470E+05	−2.599249154595520E+05	−3.653E−09
		^{1}H	−5.198494928548661E+05	−5.198494928703172E+05	−2.972E−09
^{69}Ga	C	^{239}Pu	−5.605653362583622E+04	−5.605653362098346E+04	−8.657E−09
		^{240}Pu	−3.535562084263106E+03	−3.535562084232378E+03	−8.691E−10
		^{69}Ga	1.957049906407847E+05	1.957049906411872E+05	2.057E−10
		^{71}Ga	−2.083982023582214E+02	−2.083982023382775E+02	−9.570E−09
		C	7.315556258991439E+05	7.315556256661692E+05	3.185E−08
		^{1}H	−6.011540254100939E+05	−6.011540254075985E+05	−4.151E−10
	^{1}H	^{239}Pu	−9.343452613888778E+03	−9.343452612815176E+03	−1.149E−08
		^{240}Pu	−5.893043087228781E+02	−5.893043087048698E+02	−3.056E−09
		^{69}Ga	3.261993184521389E+04	3.261993184528066E+04	2.047E−10
		^{71}Ga	−3.473562495944646E+01	−3.473562495473440E+01	−1.357E−08
		C	−5.009993875531397E+04	−5.009993874885706E+04	−1.289E−08
		^{1}H	9.319330217380848E+05	9.319330214754802E+05	2.818E−08
^{71}Ga	^{71}Ga	^{239}Pu	−7.409714869784210E+04	−7.409714869205316E+04	−7.813E−09
		^{240}Pu	−4.673408299498435E+03	−4.673408300100544E+03	−1.288E−08
		^{69}Ga	−4.150987133933455E+02	−4.150987133711392E+02	−5.350E−09
		^{71}Ga	3.455683398110428E+05	3.455683398009285E+05	2.927E−09
		C	−2.599249154690470E+05	−2.599249154709368E+05	−7.271E−10
		^{1}H	−5.198494928548661E+05	−5.198494928892467E+05	−6.614E−09
	C	^{239}Pu	−5.605653362583622E+04	−5.605653363279794E+04	−1.242E−08
		^{240}Pu	−3.535562084263106E+03	−3.535562084801918E+03	−1.524E−08
		^{69}Ga	−3.140336085031174E+02	−3.140336085762294E+02	−2.328E−08
		^{71}Ga	1.958106260469295E+05	1.958106260471490E+05	1.121E−10
		C	7.315556258991439E+05	7.315556257116593E+05	2.563E−08
		^{1}H	−6.011540254100939E+05	−6.011540256023979E+05	−3.199E−08
	^{1}H	^{239}Pu	−9.343452613888778E+03	−9.343452614741347E+03	−9.125E−09
		^{240}Pu	−5.893043087228781E+02	−5.893043087791624E+02	−9.551E−09
		^{69}Ga	−5.234283945921759E+01	−5.234283947275009E+01	−2.585E−08
		^{71}Ga	3.263753905971366E+04	3.263753905975100E+04	1.144E−10
		C	−5.009993875531397E+04	−5.009993876661654E+04	−2.256E−08
		^{1}H	9.319330217380848E+05	9.319330215125590E+05	2.420E−08
C	C	^{239}Pu	−6.482378323511393E+04	−6.482378419895817E+04	−1.487E−06
		^{240}Pu	−4.088524483057356E+03	−4.088524543853756E+03	−1.487E−06
		^{69}Ga	−3.631485082902867E+02	−3.631485136897144E+02	−1.487E−06
		^{71}Ga	−2.409917100195159E+02	−2.409917136027583E+02	−1.487E−06
		C	4.054769251876398E+06	4.054769383954272E+06	3.257E−06
		^{1}H	−1.417115856806510E+06	−1.417115878898552E+06	−1.559E−06
	^{1}H	^{239}Pu	−1.080476989449684E+04	−1.080477005514780E+04	−1.487E−06
		^{240}Pu	−6.814715840824639E+02	−6.814715942158971E+02	−1.487E−06
		^{69}Ga	−6.052926678739268E+01	−6.052926768735639E+01	−1.487E−06
		^{71}Ga	−4.016828150554025E+01	−4.016828210279664E+01	−1.487E−06
		C	2.788717086938128E+05	2.788717247445498E+05	5.756E−06
		^{1}H	2.145460223924732E+06	2.145460256022408E+06	1.496E−06
^{1}H	^{1}H	^{239}Pu	−1.800929329434564E+03	−1.800929332412145E+03	−1.653E−07
		^{240}Pu	−1.135870707968922E+02	−1.135870709849643E+02	−1.656E−07
		^{69}Ga	−1.008896375498992E+01	−1.008896377166299E+01	−1.653E−07
		^{71}Ga	−6.695213038563294E+00	−6.695213049630595E+00	−1.653E−07
		C	−1.968511433715311E+04	−1.968511437120866E+04	−1.730E−07
		^{1}H	7.545769645520820E+05	7.545769671355219E+05	3.424E−07

TABLE B.XV

Third Derivatives of L with Respect to N_i, σ_j, and σ_k

Isotope			$\partial^3 L/\partial N_i \partial\sigma_j \partial\sigma_k$ (cm/atom · b · s)		
i	j	k	Multidual	Central Difference	Difference (%)
^{239}Pu	^{239}Pu	^{239}Pu	2.311554020212181E+02	2.311556144683682E+02	9.191E−05
		^{240}Pu	−4.721993565522159E+01	−4.721995539252353E+01	−4.180E−05
		^{69}Ga	−4.194141252135556E+00	−4.194143005230790E+00	−4.180E−05
		^{71}Ga	−2.783305588047693E+00	−2.783306751432838E+00	−4.180E−05
		C	7.997679485464885E+02	7.997687127275267E+02	9.555E−05
		^{1}H	1.599534856838220E+03	1.599536385199694E+03	9.555E−05
	^{240}Pu	^{240}Pu	−6.875987089772191E+00	−6.875997300601164E+00	−1.485E−04
		^{69}Ga	−6.107348665812089E−01	−6.107357735214675E−01	−1.485E−04
		^{71}Ga	−4.052943534282532E−01	−4.052949552897147E−01	−1.485E−04
		C	−2.743851256195888E+02	−2.743853020627363E+02	−6.430E−05
		^{1}H	−5.487698943476156E+02	−5.487702472336891E+02	−6.430E−05
	^{69}Ga	^{69}Ga	−5.424633181943988E−02	−5.424641237515103E−02	−1.485E−04
		^{71}Ga	−3.599881582606673E−02	−3.599886928425081E−02	−1.485E−04
		C	−2.437127366577122E+01	−2.437128933770051E+01	−6.430E−05
		^{1}H	−4.874251563193079E+01	−4.874254697576842E+01	−6.430E−05
	^{71}Ga	^{71}Ga	−2.388944463917952E−02	−2.388948011496667E−02	−1.485E−04
		C	−1.617320402531556E+01	−1.617321442548181E+01	−6.430E−05
		^{1}H	−3.234638701421367E+01	−3.234640781453259E+01	−6.430E−05
	C	C	4.162212808543174E+03	4.162216974436882E+03	1.001E−04
		^{1}H	8.324420203313912E+03	8.324428535128585E+03	1.001E−04
	^{1}H	^{1}H	1.664882957909000E+04	1.664884624268826E+04	1.001E−04
^{240}Pu	^{239}Pu	^{239}Pu	−2.708334927885626E+03	−2.708334957841025E+03	−1.106E−06
		^{240}Pu	8.090117296097209E+02	8.090117474602549E+02	2.206E−06
		^{69}Ga	−1.517232935086371E+01	−1.517232951864096E+01	−1.106E−06
		^{71}Ga	−1.006862347434221E+01	−1.006862358567184E+01	−1.106E−06
		C	−9.500550825014945E+03	−9.500550888112177E+03	−6.641E−07
		^{1}H	−1.900108929270397E+04	−1.900108941887326E+04	−6.640E−07
	^{240}Pu	^{240}Pu	1.128246963141303E+02	1.128246879112393E+02	7.448E−06
		^{69}Ga	4.532154529326717E+00	4.532154629327612E+00	2.206E−06
		^{71}Ga	3.007617118509733E+00	3.007617184872887E+00	2.207E−06
		C	4.550946679467395E+03	4.550947727450456E+03	1.054E−06
		^{1}H	9.101887439537866E+03	9.101887535504595E+03	1.054E−06
	^{69}Ga	^{69}Ga	−8.499671719361362E−02	−8.499671813352710E−02	−1.106E−06
		^{71}Ga	−5.640531010018749E−02	−5.640531072385390E−02	−1.106E−06
		C	−5.322291739016184E+01	−5.322291774362884E+01	−6.641E−07
		^{1}H	−1.064457655535021E+02	−1.064457662602980E+02	−6.640E−07
	^{71}Ga	^{71}Ga	−3.743155162394161E−02	−3.743155203781939E−02	−1.106E−06
		C	−3.531966008746402E+01	−3.531966032202150E+01	−6.641E−07
		^{1}H	−7.063927423479689E+01	−7.063927470384608E+01	−6.640E−07
	C	C	−5.094230517822391E+04	−5.094230534763521E+04	−3.326E−07
		^{1}H	−1.018845440960090E+05	−1.018845444348295E+05	−3.326E−07
	^{1}H	^{1}H	−2.037689556712261E+05	−2.037689563484660E+05	−3.324E−07
^{69}Ga	^{239}Pu	^{239}Pu	−4.198578431892845E+02	−4.198578431866535E+02	−6.266E−10
		^{240}Pu	−2.648100721084099E+01	−2.648100721266487E+01	−6.888E−09
		^{69}Ga	9.774780295774789E+02	9.774780295812253E+02	3.833E−10
		^{71}Ga	−1.560881740399296E+00	−1.560881740606253E+00	−1.326E−08
		C	−1.472816651083490E+03	−1.472816650964507E+03	−8.079E−09

(Continued)

TABLE B.XV (Continued)

Isotope			$\partial^3 L/\partial N_i \partial\sigma_j \partial\sigma_k$ (cm/atom · b · s)		
i	*j*	*k*	Multidual	Central Difference	Difference (%)
		^{1}H	−2.945631386480648E+03	−2.945631386624474E+03	−4.883E−09
	^{240}Pu	^{240}Pu	−1.670193267258964E+00	−1.670193267349374E+00	−5.413E−09
		^{69}Ga	6.165087343148736E+01	6.165087343171735E+01	3.730E−10
		^{71}Ga	−9.844694172867779E−02	−9.844694174298671E−02	−1.453E−08
		C	−9.289255635032981E+01	−9.289255634304079E+01	−7.847E−09
		^{1}H	−1.857849918757080E+02	−1.857849918841492E+02	−4.544E−09
	^{69}Ga	^{69}Ga	1.096501153847646E+01	1.096501152534108E+01	1.198E−07
		^{71}Ga	3.633914746999563E+00	3.633914747011708E+00	3.342E−10
		C	5.141908538972495E+03	5.141908538984124E+03	2.262E−10
		^{1}H	1.028381038988650E+04	1.028381038990738E+04	2.030E−10
	^{71}Ga	^{71}Ga	−5.802801703083962E−03	−5.802801704050880E−03	−1.666E−08
		C	−5.475407104865853E+00	−5.475407104452347E+00	−7.552E−09
		^{1}H	−1.095080708789305E+01	−1.095080708838557E+01	−4.498E−09
	C	C	−7.897297398116582E+03	−7.897297397533101E+03	−7.388E−09
		^{1}H	−1.579458452425215E+04	−1.579458452460845E+04	−2.256E−09
	^{1}H	^{1}H	−3.158914850455560E+04	−3.158914850479614E+04	−7.615E−10
^{71}Ga	^{239}Pu	^{239}Pu	−4.198578431892845E+02	−4.198578431569723E+02	−7.696E−09
		^{240}Pu	−2.648100721084099E+01	−2.648100721378863E+01	−1.113E−08
		^{69}Ga	−2.352080391469268E+00	−2.352080391216942E+00	−1.073E−08
		^{71}Ga	9.782692282285486E+02	9.782692282299914E+02	1.475E−10
		C	−1.472816651083490E+03	−1.472816651100147E+03	−1.131E−09
		^{1}H	−2.945631386480648E+03	−2.945631386788828E+03	−1.046E−08
	^{240}Pu	^{240}Pu	−1.670193267258964E+00	−1.670193267460508E+00	−1.207E−08
		^{69}Ga	−1.483489205152117E−01	−1.483489205065495E−01	−5.839E−09
		^{71}Ga	6.170077541027391E+01	6.170077541036382E+01	1.457E−10
		C	−9.289255635032981E+01	−9.289255634726874E+01	−3.295E−09
		^{1}H	−1.857849918757080E+02	−1.857849918980833E+02	−1.204E−08
	^{69}Ga	^{69}Ga	−1.317656025170430E−02	−1.317656025097632E−02	−5.525E−09
		^{71}Ga	5.480349853216384E+00	5.480349853224317E+00	1.448E−10
		C	−8.250847808221488E+00	−8.250847807920774E+00	−3.645E−09
		^{1}H	−1.650168488460045E+01	−1.650168488534263E+01	−4.498E−09
	^{71}Ga	^{71}Ga	7.279515084591429E+00	7.279515078800185E+00	7.956E−08
		C	5.144683979675849E+03	5.144683979681446E+03	1.088E−10
		^{1}H	1.028936126768321E+04	1.028936126769300E+04	9.514E−11
	C	C	−7.897297398116582E+03	−7.897297400254674E+03	−2.707E−08
		^{1}H	−1.579458452425215E+04	−1.579458452687873E+04	−1.663E−08
	^{1}H	^{1}H	−3.158914850455560E+04	−3.158914851706038E+04	−3.959E−08
C	^{239}Pu	^{239}Pu	−3.176340212602082E+02	−3.176340257732987E+02	−1.421E−06
		^{240}Pu	−2.003361124209830E+01	−2.003361152675518E+01	−1.421E−06
		^{69}Ga	−1.779413592454560E+00	−1.779413617738543E+00	−1.421E−06
		^{71}Ga	−1.180850023304541E+00	−1.180850040082144E+00	−1.421E−06
		C	4.145225189642776E+03	4.145225416479916E+03	5.472E−06
		^{1}H	−3.406328542579788E+03	−3.406328593228896E+03	−1.487E−06
	^{240}Pu	^{240}Pu	−1.263547203813983E+00	−1.263547221767809E+00	−1.421E−06
		^{69}Ga	−1.122300438999165E−01	−1.122300454945726E−01	−1.421E−06
		^{71}Ga	−7.447782264710917E−02	−7.447782370528734E−02	−1.421E−06
		C	2.614450103007903E+02	2.614450246077318E+02	5.472E−06
		^{1}H	−2.148417902911072E+02	−2.148417934856076E+02	−1.487E−06

(Continued)

TABLE B.XV (Continued)

Isotope			$\partial^3 L/\partial N_i \partial\sigma_j \partial\sigma_k$ (cm/atom · b · s)		
i	j	k	Multidual	Central Difference	Difference (%)
	^{69}Ga	^{69}Ga	−9.968430712962502E−03	−9.968430854605562E−03	−1.421E−06
		^{71}Ga	−6.615225200946120E−03	−6.615225294935146E−03	−1.421E−06
		C	2.322191438111996E+01	2.322191565188290E+01	5.472E−06
		^{1}H	−1.908255068202210E+01	−1.908255096576113E+01	−1.487E−06
	^{71}Ga	^{71}Ga	−4.389979297576650E−03	−4.389979359948780E−03	−1.421E−06
		C	1.541046907498084E+01	1.541046991828117E+01	5.472E−06
		^{1}H	−1.266351483046306E+01	−1.266351501875520E+01	−1.487E−06
	C	C	1.065340877180544E+05	1.065340744519607E+05	1.245E−05
		^{1}H	8.791752812112679E+04	8.791753318130737E+04	5.756E−06
	^{1}H	^{1}H	−7.446591282206490E+04	−7.446591398296764E+04	−1.559E−06
^{1}H	^{239}Pu	^{239}Pu	−5.294295301976802E+01	−5.294295310327021E+01	−1.577E−07
		^{240}Pu	−3.339184305883357E+00	−3.339184311157747E+00	−1.580E−07
		^{69}Ga	−2.965910573882862E−01	−2.965910578560713E−01	−1.577E−07
		^{71}Ga	−1.968230199623024E−01	−1.968230202728745E−01	−1.578E−07
		C	−2.838820737286205E+02	−2.838820741974350E+02	−1.651E−07
		^{1}H	5.280626790369602E+03	5.280626817453849E+03	5.129E−07
	^{240}Pu	^{240}Pu	−2.106069116411852E−01	−2.106069119736965E−01	−1.579E−07
		^{69}Ga	−1.870640279031140E−02	−1.870640281981691E−02	−1.577E−07
		^{71}Ga	−1.241389650194405E−02	−1.241389652154238E−02	−1.579E−07
		C	−1.790482984510305E+01	−1.790482987467140E+01	−1.651E−07
		^{1}H	3.330563389058689E+02	3.330563406140848E+02	5.129E−07
	^{69}Ga	^{69}Ga	−1.661529066764682E−03	−1.661529069385245E−03	−1.577E−07
		^{71}Ga	−1.102619787513144E−03	−1.102619789253465E−03	−1.578E−07
		C	−1.590332227771904E+00	−1.590332230398922E+00	−1.652E−07
		^{1}H	2.958253354027762E+01	2.958253369200510E+01	5.129E−07
	^{71}Ga	^{71}Ga	−7.317178014723933E−04	−7.317178026279780E−04	−1.579E−07
		C	−1.055372318268031E+00	−1.055372320010401E+00	−1.651E−07
		^{1}H	1.963148734424218E+01	1.963148744493140E+01	5.129E−07
	C	C	−3.102981881787979E+03	−3.102981887154940E+03	−1.730E−07
		^{1}H	5.636933534144331E+04	5.636933564408496E+04	5.369E−07
	^{1}H	^{1}H	2.378891061100814E+05	2.378890949302082E+05	4.700E−06

TABLE B.XVI

Third Derivatives of L with Respect to σ_i, σ_j, and σ_k

Isotope			$\partial^3 L/\partial\sigma_i \partial\sigma_j \partial\sigma_k$ (/b^3 · s)		
i	j	k	Multidual	Central Difference	Difference (%)
^{239}Pu	^{239}Pu	^{239}Pu	−2.379047123748252E+00	−2.379053737401764E+00	−2.780E−04
		^{240}Pu	−1.500497491254651E−01	−1.500501662576081E−01	−2.780E−04
		^{69}Ga	−1.332763024657205E−02	−1.332766748649477E−02	−2.794E−04
		^{71}Ga	−8.844448842020021E−03	−8.844473429223933E−03	−2.780E−04
		C	−8.345444236442320E+00	−8.345458167941588E+00	−1.669E−04
		^{1}H	−1.669087761800095E+01	−1.669090548097855E+01	−1.669E−04
	^{240}Pu	^{240}Pu	−9.463842471999041E−03	−9.463868781091183E−03	−2.780E−04
		^{69}Ga	−8.405918298013587E−04	−8.405941666120432E−04	−2.780E−04

(Continued)

TABLE B.XVI (Continued)

Isotope			$\partial^3 L/\partial\sigma_i\partial\sigma_j\partial\sigma_k$ (/b^3 · s)		
i	*j*	*k*	Multidual	Central Difference	Difference (%)
		^{71}Ga	−5.578314597682723E−04	−5.578330105168082E−04	−2.780E−04
		C	−5.263585582305625E−01	−5.263594369091946E−01	−1.669E−04
		^{1}H	−1.052716431828795E+00	−1.052718170219070E+00	−1.651E−04
	^{69}Ga	^{69}Ga	−7.466255132831193E−05	−7.466275888712877E−05	−2.780E−04
		^{71}Ga	−4.954737664693019E−05	−4.954751438659808E−05	−2.780E−04
		C	−4.675190916413517E−02	−4.675198720960884E−02	−1.669E−04
		^{1}H	−9.350375751826157E−02	−9.350391360910482E−02	−1.669E−04
	^{71}Ga	^{71}Ga	−3.288050687951642E−05	−3.288059828597292E−05	−2.780E−04
		C	−3.102538570015458E−02	−3.102543749249663E−02	−1.669E−04
		^{1}H	−6.205073104572242E−02	−6.205083463034012E−02	−1.669E−04
	C	C	−4.474858089504539E+01	−4.474861829652234E+01	−8.358E−05
		^{1}H	−8.949710358580262E+01	−8.949717838869097E+01	−8.358E−05
	^{1}H	^{1}H	−1.789940907631046E+02	−1.789942403687780E+02	−8.358E−05
^{240}Pu	^{240}Pu	^{240}Pu	−5.968974613873462E−04	−5.968974679884927E−04	−1.106E−06
		^{69}Ga	−5.301727398315470E−05	−5.301727456944738E−05	−1.106E−06
		^{71}Ga	−3.518319152108287E−05	−3.518319191584935E−05	−1.122E−06
		C	−3.319815266546514E−02	−3.319815288604753E−02	−6.644E−07
		^{1}H	−6.639626215023479E−02	−6.639626259120997E−02	−6.642E−07
	^{69}Ga	^{69}Ga	−4.709069015089172E−06	−4.709069067167253E−06	−1.106E−06
		^{71}Ga	−3.125020669612918E−06	−3.125039670013810E−06	−6.080E−04
		C	−2.948706720093125E−03	−2.948706739669897E−03	−6.639E−07
		^{1}H	−5.897409604816003E−03	−5.897409643801863E−03	−6.611E−07
	^{71}Ga	^{71}Ga	−2.073818445687669E−06	−2.073818468617714E−06	−1.106E−06
		C	−1.956813420952389E−03	−1.956813433948622E−03	−6.642E−07
		^{1}H	−3.913624296685913E−03	−3.913624322672628E−03	−6.640E−07
	C	C	−2.822354071928983E+00	−2.822354081319165E+00	−3.327E−07
		^{1}H	−5.644704472834071E+00	−5.644704491614327E+00	−3.327E−07
	^{1}H	^{1}H	−1.128940160362512E+01	−1.128940164111165E+01	−3.321E−07
^{69}Ga	^{69}Ga	^{69}Ga	−4.182661484240016E−07	−4.182661484219589E−07	−4.884E−10
		^{71}Ga	−2.775687413023951E−07	−2.775687413069558E−07	−1.643E−09
		C	−2.619082877514298E−04	−2.619082877246118E−04	−1.024E−08
		^{1}H	−5.238162348398675E−04	−5.238162347976234E−04	−8.065E−09
	^{71}Ga	^{71}Ga	−1.841994778647366E−07	−1.841994778954295E−07	−1.666E−08
		C	−1.738069266225554E−04	−1.738069266026389E−04	−1.146E−08
		^{1}H	−3.476136271751831E−04	−3.476136271093234E−04	−1.895E−08
	C	C	−2.506854674186975E−01	−2.506854673723586E−01	−1.848E−08
		^{1}H	−5.013706087718773E−01	−5.013706086719190E−01	−1.994E−08
	^{1}H	^{1}H	−1.002740565413143E+00	−1.002740565309510E+00	−1.033E−08
^{71}Ga	^{71}Ga	^{71}Ga	−1.222379994463332E−07	−1.222379994334025E−07	−1.058E−08
		C	−1.153413204344606E−04	−1.153413204467566E−04	−1.066E−08
		^{1}H	−2.306824908449580E−04	−2.306824908601171E−04	−6.571E−09
	C	C	−1.663592665014656E−01	−1.663592665465053E−01	−2.707E−08
		^{1}H	−3.327183166201432E−01	−3.327183167311077E−01	−3.335E−08
	^{1}H	^{1}H	−6.654362004749920E−01	−6.654362004046038E−01	−1.058E−08
C	C	C	−4.891257624311546E+02	−4.891257700560944E+02	−1.559E−06
		^{1}H	−9.782508886585181E+02	−9.782509039084024E+02	−1.559E−06
	^{1}H	^{1}H	−1.956500504910280E+03	−1.956500535410990E+03	−1.559E−06
^{1}H	^{1}H	^{1}H	−3.912998465008702E+03	−3.912998471796426E+03	−1.735E−07

Acknowledgments

This material was partially funded by the CONsortium on Nuclear sECurity Technologies (CONNECT), which is funded by the U.S. Department of Energy National Nuclear Security Administration under award number DE-NA0003948. The authors would like to thank Louse Mendius (Los Alamos National Laboratory) for the drawing in Fig. 1.

ORCID

Matthew R. Balcer http://orcid.org/0000-0002-7864-9518

References

1. G. LANTOINE, R. P. RUSSELL, and T. DARGENT, "Using Multicomplex Variables for Automatic Computation of High-Order Derivatives," *ACM Trans. Math. Software*, **38**, *3*, 1 (2012); https://doi.org/10.1145/2168773.2168774.
2. J. A. FIKE and J. J. ALONSO, "The Development of Hyper-Dual Numbers for Exact Second-Derivative Calculations," presented at the 49th AIAA Aerospace Sciences Mtg. and New Horizons Forum and Aerospace Exposition, p. 886, American Institute of Aeronautics and Astronautics (2011); https://doi.org/10.2514/6.2011-886.
3. W. SQUIRE and G. TRAPP, "Using Complex Variables to Estimate Derivatives of Real Functions," *SIAM Rev.*, **40**, *1*, 110 (1998); https://doi.org/10.1137/s003614459631241x.
4. A. M. AGUIRRE-MESA et al., "A Stiffness Derivative Local Hypercomplex-Variable Finite Element Method for Computing the Energy Release Rate," *Eng. Fract. Mech.*, **218**, *106581*, 106581 (2019); https://doi.org/10.1016/j.engfracmech.2019.106581.
5. V. VITTALDEV et al., "Second-Order Kalman Filters Using Multi-Complex Step Derivatives," *Proc. 22nd AAS/AIAA Space Flight Mechanics Meeting*, 1**43**, 1517, Advances in Astronautical Sciences and American Institute of Aeronautics and Astronautics, February 2, 2012 (2012).
6. M. ALEXE et al., "Automatic Differentiation of Codes in Nuclear Engineering Applications." ANL/MCS-TM-31, Argonne National Laboratory (2009); https://doi.org/10.2172/971984.
7. Z. WU and J. C. NEWMAN III, "Application of Complex-Step Derivative Method for *k*-Eigenvalue Sensitivity Calculation in Neutron Transport Models," *Ann. Nucl. Energy*, **151**, 107975 (2021); https://doi.org/10.1016/j.anucene.2020.107975.
8. P. M. BOKOV et al., "Demonstration of Prospective Application of the Dual Number Automatic Differentiation for Uncertainty Propagation in Neutronic Calculations," *Ann. Nucl. Energy*, **151**, 107925 (2021); https://doi.org/10.1016/j.anucene.2020.107925.
9. D. G. CACUCI and J. A. FAVORITE, "Second-Order Sensitivity Analysis of Uncollided Particle Contributions to Radiation Detector Responses," *Nucl. Sci. Eng.*, **190**, *2*, 105 (2018); https://doi.org/10.1080/00295639.2018.1426899.
10. D. G. CACUCI, R. FANG, and J. A. FAVORITE, "Comprehensive Second-Order Adjoint Sensitivity Analysis Methodology (2nd-aASAM) Applied to a Subcritical Experimental Reactor Physics Benchmark: I. Effects of Imprecisely Known Microscopic Total and Capture Cross Sections," *Energies*, **12**, *21*, 4219 (2019); https://doi.org/10.3390/en12214219.
11. J. A. FAVORITE, "Second-Order Sensitivity Analysis of Uncollided Particle Contributions to Radiation Detector Responses Using Ray-Tracing," *Ann. Nucl. Energy*, **127**, 490 (2019); https://doi.org/10.1016/j.anucene.2018.11.028.
12. D. G. CACUCI, "Towards Overcoming the Curse of Dimensionality: The Third-Order Adjoint Method for Sensitivity Analysis of Response-Coupled Linear Forward/Adjoint Systems, with Applications to Uncertainty Quantification and Predictive Modeling," *Energies*, **12**, *21*, 4216 (2019); https://doi.org/10.3390/en12214216.
13. H. H. TAN and K. H. LIM, "Review of Second-Order Optimization Techniques in Artificial Neural Networks Backpropagation," *IOP Conf. Ser.: Mater. Sci. Eng.*, **495**, 012003 (2019); https://doi.org/10.1088/1757-899X/495/1/012003.
14. G. GUNDERSEN and T. STEIHAUG, "On Large-Scale Unconstrained Optimization Problems and Higher Order Methods," *Optim. Methods Softw.*, **25**, *3*, 337 (2010); https://doi.org/10.1080/10556780903239071.
15. J. W. TUKEY, "The Propagation of Errors, Fluctuations, and Tolerances Basic Generalized Formulas," Technical Report No. 10, Statistical Techniques Research Group, Department of Mathematics, Princeton University (1957).
16. A. PAUDEL et al., "Higher-Order Taylor Series Expansion with Efficient Sensitivity Estimation for Uncertainty Analysis," presented at the AIAA AVIATION 2020 FORUM, American Institute of Aeronautics and Astronautics (2020); https://doi.org/10.2514/6.2020-3164.
17. W. H. PRESS et al., *Numerical Recipes: The Art of Scientific Computing*, Cambridge University Press (2007).
18. J. IOTT, R. T. HAFTKA, and H. M. ADELMAN, "Selecting Step Sizes in Sensitivity Analysis by Finite Differences," NASA-TM-86382, National Aeronautics and Space Administration (1985).
19. J. R. R. A. MARTINS, P. STURDZA, and J. J. ALONSO, "The Complex-Step Derivative Approximation," *ACM*

Trans. Math. Software, **29**, *3*, 245 (2003); https://doi.org/10.1145/838250.838251.

20. I. L. KANTOR and A. S. SOLODOVNIKOV, *Hypercomplex Numbers: An Elementary Introduction to Algebras*, Springer-Verlag, New York (1989).

21. M. S. P. EASTHAM, "2968. On the Definition of Dual Numbers," *Math. Gazette*, **45**, *353*, 232 (1961); https://doi.org/10.2307/3612794.

22. A. M. AGUIRRE-MESA, M. J. GARCIA, and H. MILLWATER, "MultiZ: A Library for Computation of High-Order Derivatives Using Multicomplex or Multidual Numbers," *ACM Trans. Math. Software*, **46**, *3*, 1 (2020); https://doi.org/10.1145/3378538.

23. J. A. FAVORITE, K. C. BLEDSOE, and D. I. KETCHESON, "Surface and Volume Integrals of Uncollided Adjoint Fluxes and Forward-Adjoint Flux Products," *Nucl. Sci. Eng.*, **163**, *1*, 73 (2009); https://doi.org/10.13182/NSE163-73.

24. R. PIESSENS et al., *Quadpack: A Subroutine Package for Automatic Integration*, Vol. 1, Springer-Verlag (1983).

25. R. E. ALCOUFFE et al., "PARTISN: A Time-Dependent, Parallel Neutral Particle Transport Code System," LA-UR-17-29704, Los Alamos National Laboratory (2019).

26. "Symbolic Math Toolbox," The MathWorks, Inc.; https://www.mathworks.com/help/symbolic/ (current as of Sep. 22, 2020).